

Original Article

Cite this article: Cucciniello C, Choudhary AK, Pande K, and Sheth H (2019) Mineralogy, geochemistry and ^{40}Ar – ^{39}Ar geochronology of the Barda and Alech complexes, Saurashtra, northwestern Deccan Traps: early silicic magmas derived by flood basalt fractionation. *Geological Magazine* **156**: 1668–1690. <https://doi.org/10.1017/S0016756818000924>

Received: 29 July 2018

Revised: 23 October 2018

Accepted: 3 December 2018


First published online: 22 January 2019

Keywords:

Ar–Ar dating; Deccan Traps; granophyre; rhyolite; petrogenesis; Saurashtra

Author for correspondence: Ciro Cucciniello,
Email: ciro.cucciniello@unina.it

Mineralogy, geochemistry and ^{40}Ar – ^{39}Ar geochronology of the Barda and Alech complexes, Saurashtra, northwestern Deccan Traps: early silicic magmas derived by flood basalt fractionation

Ciro Cucciniello¹ , Ashwini Kumar Choudhary², Kanchan Pande³ and Hetu Sheth³

¹Dipartimento di Scienze della Terra, dell'Ambiente e delle Risorse (DiSTAR), Università di Napoli Federico II, Complesso Universitario Monte Sant'Angelo, Via Cintia 26 (edificio L), 80126 Napoli, Italy; ²Institute Instrumentation Center, Indian Institute of Technology Roorkee, Roorkee 247667, India and ³Department of Earth Sciences, Indian Institute of Technology Bombay, Powai, Mumbai 400076, India

Abstract

Most continental flood basalt (CFB) provinces of the world contain silicic (granitic and rhyolitic) rocks, which are of significant petrogenetic interest. These rocks can form by advanced fractional crystallization of basaltic magmas, crustal assimilation with fractional crystallization, partial melting of hydrothermally altered basaltic lava flows or intrusions, anatexis of old basement crust, or hybridization between basaltic and crustal melts. In the Deccan Traps CFB province of India, the Barda and Alech Hills, dominated by granophyre and rhyolite, respectively, form the largest silicic complexes. We present petrographic, mineral chemical, and whole-rock geochemical (major and trace element and Sr–Nd isotopic) data on rocks of both complexes, along with ^{40}Ar – ^{39}Ar ages of 69.5–68.5 Ma on three Barda granophyres. Whereas silicic magmatism in the Deccan Traps typically postdates flood basalt eruptions, the Barda granophyre intrusions (and the Deccan basalt flows they intrude) significantly pre-date (by 3–4 My) the intense 66–65 Ma flood basalt phase forming the bulk of the province. A tholeiitic dyke cutting the Barda granophyres contains quartzite xenoliths, the first being reported from Saurashtra and probably representing Precambrian basement crust. However, geochemical–isotopic data show little involvement of ancient basement crust in the genesis of the Barda–Alech silicic rocks. We conclude that these rocks formed by advanced (70–75%), nearly-closed system fractional crystallization of basaltic magmas in crustal magma chambers. The sheer size of each complex (tens of kilometres in diameter) indicates a very large mafic magma chamber, and a wide, pronounced, circular-shaped gravity high and magnetic anomaly mapped over these complexes is arguably the geophysical signature of this solidified magma chamber. The Barda and Alech complexes are important for understanding CFB-associated silicic magmatism, and anorogenic, intraplate silicic magmatism in general.

1. Introduction

Silicic (granitic and rhyolitic) rocks are found in most continental flood basalt (CFB) provinces of the world, sometimes in volumetrically significant amounts. Notable volumes of rhyolite, for example, occur in the Karoo and Paraná CFB provinces (e.g. Cleverly *et al.* 1984; Garland *et al.* 1995) and in the Snake River Plain 'hotspot track' associated with the Columbia River CFB province (e.g. Ellis *et al.* 2013). The Deccan Traps CFB province of India, though poor in silicic rocks overall, has significant concentrations of these rocks in its western and northwestern parts, along the western Indian rifted margin. As in many other rifted-margin CFB provinces like the Karoo (Melluso *et al.* 2008), silicic magmatism in the Deccan generally postdates thick flood basalt sequences (e.g. Sheth & Melluso, 2008; Owen-Smith *et al.* 2013; Sheth & Pande, 2014; Shellnutt *et al.* 2017).

The Barda Hills (dominantly composed of granophyre) and Alech Hills (dominantly rhyolite) in Saurashtra, NW Deccan Traps, form the largest silicic complexes in the entire province (Fig. 1a, b). Each complex covers several tens of kilometres in diameter. Yet there has been no focused study of the Barda complex since those by Dave (1971) and De & Bhattacharyya (1971), and almost no geological, petrological or geochemical information on the Alech complex is available in the otherwise vast Deccan Traps literature. The petrogenesis of silicic rocks in CFB provinces is a topic of considerable interest, and we have carried out a mineralogical and geochemical–isotopic study of select Barda–Alech silicic rocks to understand their petrogenetic evolution. We have also dated, by the ^{40}Ar – ^{39}Ar incremental heating technique, three of the Barda granophyres. The combined results show that the silicic rocks are products of

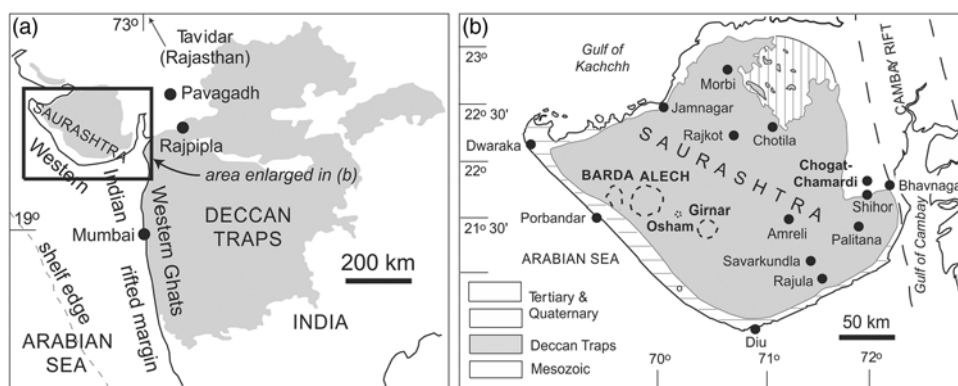


Fig. 1. Simplified geological maps of the Deccan Traps (a) and of Saurashtra (b), with the important central complexes and locations in Saurashtra marked (after De, 1981; Misra, 1981).

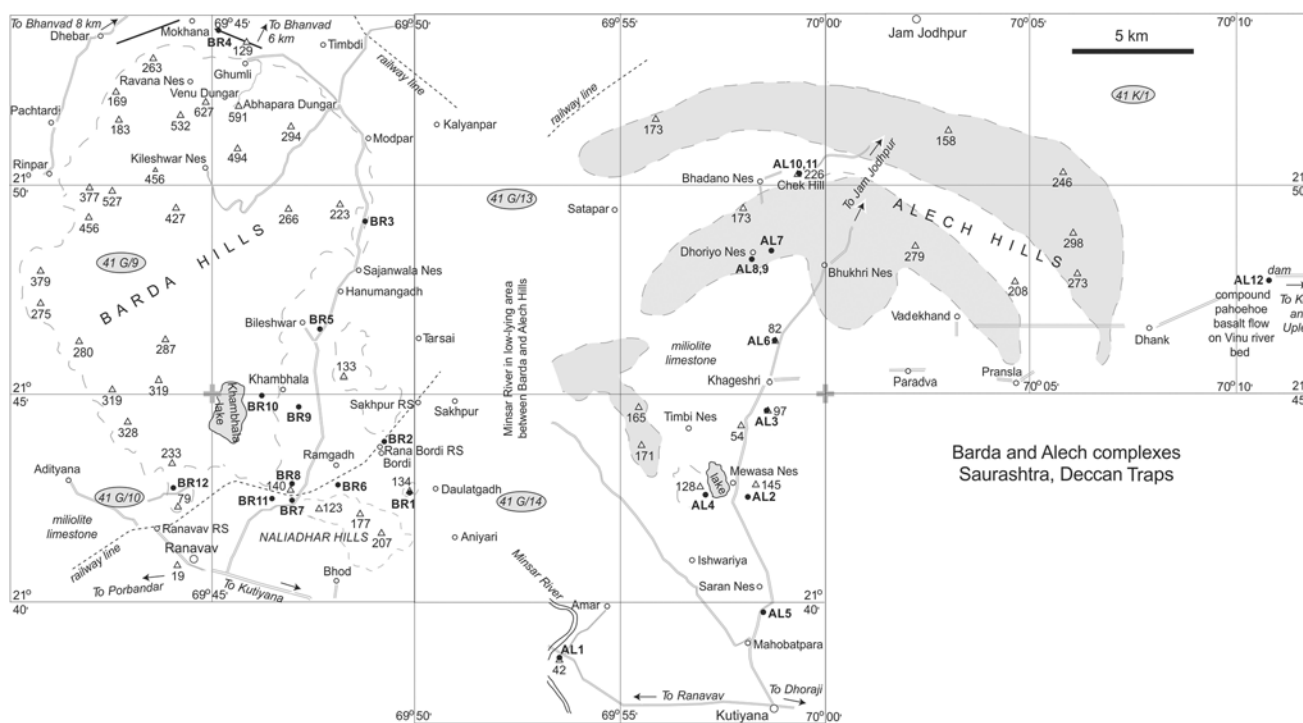


Fig. 2. Topography and localities in the Barda and Alech complexes, Saurashtra, with the sample locations marked. Numbers within grey ellipses are the numbers of the Survey of India topographic sheets of 1:50,000 scale, and numbers near triangles are the elevations of points above mean sea level.

fractional crystallization of early basaltic magmas, with little or no input from pre-existing crust, and, in contrast to the general observation in CFB provinces, the Barda granophyre plutons significantly pre-date the main (66–65 Ma) Deccan CFB eruptions.

2. Geological background

The large (present-day areal extent 500,000 km²) Deccan Traps CFB province in west-central India is made up of flat-lying flood tholeiite lavas reaching a stratigraphic thickness of 3.5 km in the Western Ghats escarpment (Fig. 1a). The Saurashtra peninsula in the NW part of the Deccan province, also covered by the Deccan lavas, is nearly flat and low-lying, with few thick vertical sections through the lavas and its coastal fringes covered by Tertiary or Quaternary limestones and alluvium. However, special features of Saurashtra’s Deccan geology, noted for a long time, include several volcano–plutonic complexes (e.g. Fedden, 1884; Adaye, 1914; Mathur *et al.* 1926; Auden, 1949), a great range of rock

types including primitive picrites (e.g. Krishnan, 1926; Chatterjee, 1932; West, 1958; Krishnamacharlu, 1972; Krishnamurthy & Cox, 1977), and an abundance of rhyolite and granophyre (e.g. Dave, 1971; De & Bhattacharyya, 1971; Subba Rao, 1971; De, 1981; Chatterjee & Bhattacharji, 2001). A large ring dyke of granophyre or silicic porphyry cuts the gabbro–diorite–monzonite plutonic complex of Mount Girnar (1117 m, Fig. 1b; Mathur *et al.* 1926). Osham Hill (314 m) to the NW of Mount Girnar exposes flows of rhyolite and pitchstone capping tholeiitic flows. These silicic rocks show spectacular flow layering and flow folding (Wakhaloo, 1967; Sheth *et al.* 2012) and appear to represent rheomorphic, lava-like ignimbrites.

The Barda Hills, near Porbandar town on the Arabian Sea and composed dominantly of granophyre, reach a substantial height of 627 m above mean sea level (amsl) (Figs. 2 and 3a). There are many individual granophyre stocks emplaced through low-lying basaltic lava flows (Dave, 1971; De & Bhattacharyya, 1971). Barda granophyres generally form rounded and massive outcrops and are



Fig. 3. (Colour online) Field photographs showing (a) imposing landscape of the granophyre hills near Porbandar, Barda complex. Building and farmers provide a scale. (b) Flow folding in brown Alech rhyolite (sample AL7) near Dhoriyo Nes. Person provides a scale.

intruded by mafic dykes in the northern parts (e.g. BR4, Fig. 2). The peripheries of the Barda Hills are occupied by the Quaternary-age Miliolite Limestone (e.g. Lele, 1973; Marathe *et al.* 1977) which provides raw material for cement factories in the area.

In comparison, the Alech Hills, dominantly composed of rhyolites, form a series of low (~150–298 m amsl) and distinctly arcuate to concentric hill ranges whose intervening depressions are also covered by Miliolite Limestone. Few exposed sections across these ranges are available. Misra (1981) has considered these arcuate hill ranges to represent ring dykes. However, we have observed a small outcrop of volcanic tuff 2 km north of Khageshri village, near the centre of the ring complex (Fig. 2). More suggestively, the rhyolite just east of Dhoriyo Nes hamlet (sample AL7, Fig. 2) shows large-scale flow layering and flow folding (Fig. 3b), and may be a rheomorphic, lava-like ignimbrite. If so, the Alech Hills rhyolites may represent large-scale ring-fracture lavas and lava-like ignimbrites like those erupted from calderas of the Snake River Plain (e.g. Coble & Mahood, 2012). The Alech rhyolites are cut by dark-coloured silicic dykes such as AL4 and AL11 (Fig. 2).

3. Petrography

The Barda granophyres (samples BR1, 2, 3, 5, 6, 7, 8, 9, 10, 11, 12) are fine- to medium-grained rocks. They exhibit well-developed granophyric texture (Fig. 4a). Some of the samples are porphyritic (e.g. BR3). The rocks are made up of alkali feldspars (often perthitic, and generally making up 50–70 % of the rock), quartz (subhedral to anhedral, making up 20–30 % of most samples), minor plagioclase, and Fe–Ti oxides. Clinopyroxene grains have been observed in some samples (BR3, BR7, BR11, BR12; Fig. 4b).

Accessory minerals are zircon, baddeleyite, titanite and fluorite. De & Bhattacharyya (1971) observed Fe-rich olivine and ferroaugite in some of the granophyres.

Basalt and dolerite dykes in the Barda Hills, with phenocrysts of olivine, plagioclase (often forming glomeroporphyritic aggregates) and clinopyroxene set in a groundmass of plagioclase, clinopyroxene and glass, have been reported by Dave (1971). A basaltic andesite dyke exposed to the north of Ghumli village (Fig. 2; our sample BR4) consists of plagioclase phenocrysts set in a fine-grained groundmass with plagioclase, clinopyroxene, orthopyroxene, quartz, alkali feldspars and opaque oxides (Fig. 4c, d). Centimetre-size quartzite xenoliths containing quartz (mode 90 %), plagioclase, orthopyroxene, alkali feldspars and magnetite, and with a granoblastic–metamorphic texture (Fig. 4c, e), are found in the dyke BR4. They may be samples of the Precambrian basement crust under Saurashtra. This is the first reported occurrence of basement xenoliths in the Deccan Traps of Saurashtra, though zircon xenocrysts from Precambrian crust are known in some Rajula silicic dykes (Chatterjee & Bhattacharji, 2004).

De & Bhattacharyya (1971) reported monzodiorite (showing a hypidiomorphic texture with plagioclase, clinopyroxene, quartz, Fe–Ti oxides and apatite) ~3 km northwest of Sajanwala Nes (Fig. 2), and small dykes of aplite west of the Naliadhar Hills in the southern part of the Barda Hills (Fig. 2). The aplites consist of anhedral equigranular quartz and alkali feldspar (commonly in a micrographic intergrowth), opaque oxides, aegirine, and traces of riebeckite. Dave (1971) and De & Bhattacharyya (1971) also reported amphibole (riebeckite) in some Barda samples, though no primary hydrous phases are observed in our Barda (and Alech) rock samples.

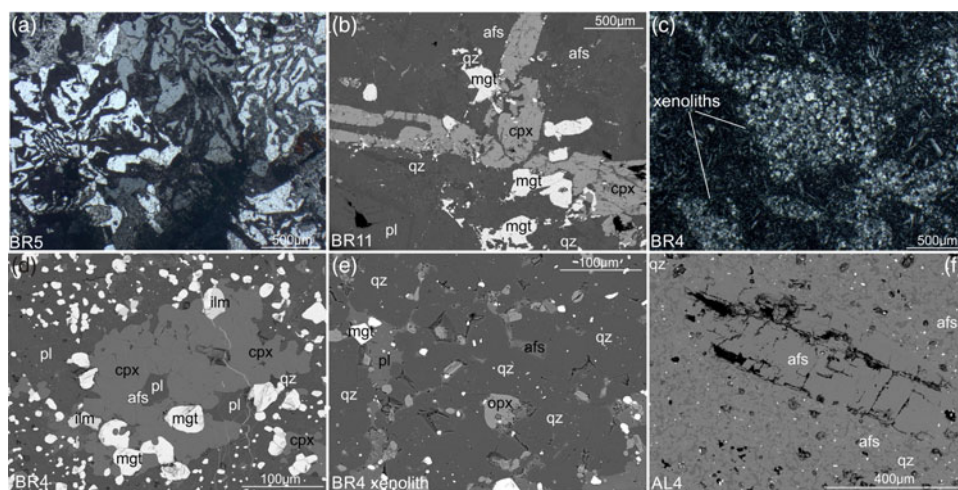
The Alech rhyolites and dacites (samples AL1, 2, 4, 5, 7, 8, 9, 10, 11) are aphyric to weakly porphyritic (up to 10 % phenocrysts). Alkali feldspar is a common phenocryst phase (Fig. 4f). Quartz occurs as phenocryst or microphenocryst in rhyolite AL9 with a fine-grained groundmass of quartz, alkali feldspars, magnetite, monazite and fluorocarbonates. Many Alech samples are visibly altered in hand specimen and under the microscope; the alteration ranges from slight alteration of alkali feldspar phenocrysts to complete replacement of alkali feldspars and mesostasis by clay, zeolites, quartz and calcite. Magnetite is partially replaced by red oxides or oxyhydroxides.

4. Analytical methods

4.a. Mineral chemical analyses

Seven rock samples from the Barda complex and nine from the Alech complex were chosen for mineral chemical analysis. Mineral compositions in the mafic rocks were determined at the University of Naples, using an Oxford Instruments Microanalysis Unit equipped with an INCA X-act detector and a JEOL JSM-5310 microscope in energy-dispersive spectrometry (EDS). The standard operating conditions included a primary beam voltage of 15 kV, filament current of 50–100 μ A and variable spot size from 30,000 to 200,000 \times magnification, 20 mm WD. Measurements were made with an INCA X-stream pulse processor and with Energy software. Energy uses the XPP matrix correction scheme developed by Pouchou & Pichoir (1988), and the pulse pile-up correction. The quant optimization is carried out using cobalt (FWHM – full width at half maximum peak height – of the strobed zero = 60–65 eV). The following standards were used for calibration: diopside (Ca), San Carlos olivine (Mg), anorthoclase (Al, Si), albite (Na), rutile (Ti), fayalite (Fe),

Fig. 4. Photomicrographs and backscattered electron (BSE) images of the Barda and Alech rocks. (a) Granophyre BR5 with typical granophyric intergrowths of quartz and alkali feldspar (crossed nicols). (b) Granophyre BR11 with alkali feldspar, quartz, plagioclase, clinopyroxene and magnetite (BSE). (c) Basaltic andesite dyke BR4 with crustal basement xenoliths (crossed nicols). (d) Groundmass of dyke BR4 with clinopyroxene, plagioclase, orthopyroxene, quartz, magnetite and ilmenite (BSE). (e) Granoblastic-polygonal texture (with quartz, orthopyroxene, plagioclase, alkali feldspar and magnetite) in quartzite basement xenolith in dyke BR4 (BSE). (f) Rhyolite AL4 with alkali feldspar microphenocryst in a groundmass of alkali feldspar and quartz (BSE). Mineral names have been abbreviated as follows: afs, alkali feldspar; cpx, clinopyroxene; opx, orthopyroxene; qz, quartz; mgt, magnetite; ilm, ilmenite; plag, plagioclase.



Cr₂O₃ (Cr), rhodonite (Mn), orthoclase (K), apatite (P), fluorite (F), barite (Ba), strontianite (Sr), zircon (Zr, Hf), synthetic Smithsonian orthophosphates (REE, Y, Sc), pure vanadium, niobium and tantalum (V, Nb, Ta), Corning glass (Th and U), sphalerite (S, Zn), galena (Pb), sodium chloride (Cl) and pollucite (Cs). The K α , L α or M α lines were used for calibration, according to the element. Backscattered electron (BSE) images were obtained with the same instrument (Fig. 4b–f). The mineral analyses are reported in Tables 1–4 and plotted in Figure 5.

4.b. ⁴⁰Ar–³⁹Ar geochronology

Three whole-rock samples of the Barda granophyres were dated using the ⁴⁰Ar–³⁹Ar incremental heating technique. Samples BR3 and BR5 were collected from low-lying outcrops on the Ranavav–Bhanvad road, north and south of Sajanwala Nes and Hanumangadh, respectively (Fig. 2). Sample BR12 was taken from the base of a jointed granophyre hillock north of Ranavav railway station (Fig. 2). None of the Alech rock samples were suitable for ⁴⁰Ar–³⁹Ar dating because of their significant alteration.

Fresh rock chips were crushed, sieved, and cleaned in deionized water in an ultrasonic bath. About 0.02 g of each was packed in aluminium capsules. Minnesota hornblende (MMhb-1, age 523.1 ± 2.6 Ma, Renne *et al.* 1998) and high-purity CaF₂ and K₂SO₄ salts were used as monitor samples. High-purity nickel wires were placed in both sample and monitor capsules to monitor the neutron fluence variation, which was typically ~5%. The aluminium capsules were kept in a 0.5 mm thick cadmium cylinder and irradiated in the heavy-water-moderated DHRUVA reactor at the Bhabha Atomic Research Centre (BARC), Mumbai, for ~100 h. The irradiated samples were repacked in aluminium foil and loaded on the extraction unit of a Thermo Fisher Scientific noble gas preparation system. Argon was extracted in a series of steps up to 1400 °C in an electrically heated ultrahigh vacuum furnace. The argon released in each step, after purification using Ti–Zr getters, was analysed with a Thermo Fisher ARGUS VI mass spectrometer, located at the National Facility for ⁴⁰Ar–³⁹Ar Geo-thermochronology in the Department of Earth Sciences, IIT Bombay. The mass spectrometer is equipped with five Faraday cups fitted with 10¹¹ Ω resistors.

Interference corrections for Ca- and K-produced Ar isotopes based on analysis of CaF₂ and K₂SO₄ salts were (³⁶Ar/³⁷Ar)_{Ca}, (³⁹Ar/³⁷Ar)_{Ca} and (⁴⁰Ar/³⁹Ar)_K = 0.000471, 0.001145 and 0.006842, respectively.

⁴⁰Ar blank contributions were 1–2% or less for all temperature steps. The irradiation parameter *J* for each sample was corrected for neutron flux variation using the activity of nickel wires irradiated with each sample. Values of fluence-corrected *J* for various samples are as follows: BR3, 0.000480 ± 0.000002; BR5, 0.000490 ± 0.000002; BR7, 0.000487 ± 0.000002; BR12, 0.000516 ± 0.000003. The plateau ages reported comprise a minimum of 50% of the total ³⁹Ar released and four or more successive degassing steps whose mean ages overlap at the 2σ level excluding the error contribution (0.5%) from the *J* value. The data were plotted using the program Isoplot/Ex v. 3.75 (Ludwig, 2012).

Table 5 gives the summary of the ⁴⁰Ar–³⁹Ar dating results (plateau, isochron and inverse isochron ages with 2σ uncertainties) for the three Barda granophyre samples. Plateau spectra and isochron plots for the three samples are shown in Figure 6. The full, stepwise analytical data are given in Supplementary Table S1 (available online at <https://doi.org/10.1017/S0016756818000924>).

4.c. Major- and trace-element analyses

The seven rock samples from the Barda complex and nine from the Alech complex analysed for mineral chemical compositions were also analysed for whole-rock major and trace element (including rare earth element (REE)) concentrations at Activation Laboratories (Actlabs), Ancaster, Ontario, Canada. Rock powders were mixed with fluxes lithium metaborate and lithium tetraborate and fused in an induction furnace. The molten samples were immediately poured into a solution of 5% nitric acid containing an internal standard and mixed continuously until completely dissolved (~30 min). The samples were analysed for major oxides and selected trace elements (Ba, Be, Sc, Sr, V, Y and Zr) on a combination simultaneous/sequential Thermo Jarrell-Ash ENVIRO II ICP or a Varian Vista 735 ICP. Calibration was performed using seven USGS and CANMET certified reference materials. One of the seven standards was used during the analysis for every group of ten samples. The fused sample solutions were diluted and analysed by a Perkin Elmer Sciex ELAN 6000, 6100 or 9000 ICP/MS for other trace elements (Cr, Co, Ni, Cu, Zn, Ga, Ge, As, Rb, Nb, Mo, Sn, Cs, La, Ce, Pr, Nd, Sm, Eu, Gd, Tb, Dy, Ho, Er, Tm, Yb, Lu, Hf, Ta, W, Pb, Bi, Th and U). Three blanks and five control samples (three before the sample group and two after) were analysed per group of samples. Duplicates were fused and analysed after every 15 samples. Analyses of international standards are reported in Table 6. The weight loss on ignition was determined

Table 1. Representative chemical analyses (in wt %) and structural formulas (in atom per formula units (apfu), calculated on basis of 32 oxygens and 20 cations) of feldspars in the Barda–Alech rocks, Saurashtra, NW Deccan Traps

Sample	Rock name	Mineral name	Description	SiO ₂	Al ₂ O ₃	FeO	CaO	Na ₂ O	K ₂ O	BaO	SrO	Sum	Si	Al	Fe	Ca	Na	K	Ba	Sr	Sum	An	Ab	Or
BR3	gph	alk-feld	gm	66.39	18.58	0.68	0.23	7.05	6.57	0.22	0.60	100.32	11.941	3.940	0.102	0.045	2.459	1.507	0.015	0.063	20.072	1	62	37
BR3	gph	alk-feld	gm	63.58	18.45	0.32	0.21	0.70	15.75	0.11	0.64	99.75	11.869	4.061	0.050	0.042	0.254	3.751	0.008	0.069	20.103	1	8	91
BR3	gph	pl	core	62.02	22.65	0.34	4.54	8.37	1.21	0.43	0.00	99.55	11.132	4.793	0.051	0.873	2.912	0.276	0.030	0.000	20.066	21	71	7
BR3	gph	pl	rim	65.13	21.21	0.48	2.33	9.81	1.16	0.27	0.36	100.75	11.500	4.416	0.071	0.441	3.358	0.261	0.019	0.036	20.102	11	82	7
BR3	gph	pl	core	62.62	22.27	0.33	4.10	8.67	1.07	0.37	0.62	100.06	11.201	4.697	0.050	0.786	3.008	0.244	0.026	0.064	20.076	19	74	7
BR7	gph	alk-feld	core	65.28	18.07	0.73	0.10	1.17	15.27	0.12	0.32	101.07	11.981	3.911	0.111	0.020	0.418	3.575	0.009	0.034	20.060	0	11	88
BR7	gph	alk feld	gm	64.40	18.16	0.09	0.15	0.80	15.92	0.09	0.28	99.90	11.962	3.977	0.014	0.031	0.288	3.771	0.006	0.031	20.080	1	8	92
BR11	gph	pl	core	64.23	21.70	–	3.69	7.69	1.81	–	0.68	99.80	11.432	4.553	0.000	0.704	2.654	0.410	0.000	0.070	19.824	18	71	11
BR11	gph	pl	rim	64.16	22.03	0.19	3.55	7.24	1.73	0.05	0.27	99.22	11.436	4.629	0.028	0.677	2.502	0.394	0.003	0.028	19.698	19	70	11
BR11	gph	alk feld	core	67.42	18.40	0.46	0.37	5.93	6.73	0.10	0.90	100.31	12.069	3.882	0.069	0.071	2.058	1.537	0.007	0.094	19.787	2	57	41
BR11	gph	alk feld	rim	67.36	18.60	0.36	0.34	5.72	7.25	–	0.65	100.27	12.055	3.924	0.054	0.065	1.983	1.654	0.000	0.067	19.802	2	54	44
BR12	gph	pl	core	61.87	22.10	0.47	4.49	8.78	1.00	–	1.04	99.75	11.137	4.689	0.070	0.866	3.064	0.230	0.000	0.108	20.166	20	74	5
BR12	gph	pl	core	63.73	22.37	0.45	4.11	8.84	0.51	–	0.43	100.44	11.271	4.664	0.067	0.778	3.030	0.116	0.000	0.044	19.970	20	77	3
BR12	gph	pl	core	64.02	21.81	0.31	3.69	9.09	1.08	0.20	0.21	100.40	11.349	4.558	0.046	0.701	3.123	0.244	0.014	0.021	20.056	17	77	6
BR4	b.a.	pl	gm	56.65	25.80	0.88	9.12	5.67	0.53	0.42	0.29	99.35	10.324	5.542	0.134	1.781	2.003	0.122	0.030	0.031	19.968	45	51	4
BR4	b.a.	alk feld	gm	63.74	18.56	0.80	0.17	1.31	14.95	0.69	0.34	100.55	11.830	4.061	0.124	0.034	0.470	3.539	0.050	0.036	20.144	1	12	87
BR4	b.a.	pl	core	47.82	32.17	0.49	16.38	2.26	–	–	0.21	99.33	8.855	7.024	0.075	3.250	0.811	0.000	0.000	0.023	20.038	80	20	0
BR4	b.a.	pl	rim	47.06	33.21	0.67	16.29	2.14	0.11	0.49	–	99.97	8.695	7.233	0.103	3.226	0.766	0.025	0.036	0.000	20.084	80	19	2
BR4	b.a.	pl	core	47.34	31.36	1.16	15.66	2.18	0.22	0.13	0.34	98.38	8.891	6.944	0.182	3.151	0.793	0.053	0.010	0.037	20.060	78	21	2
BR4	b.a.	pl	rim	56.69	26.70	0.83	9.23	5.33	0.69	0.53	0.00	100.00	10.250	5.690	0.126	1.788	1.870	0.158	0.037	0.000	19.919	46	49	5
BR4	b.a.	pl	gm	55.14	27.87	0.85	10.62	5.47	0.50	–	0.36	100.81	9.942	5.924	0.128	2.051	1.911	0.114	0.000	0.038	20.109	50	47	3
BR4	xen	pl	core	51.64	29.20	0.41	13.26	3.87	0.16	–	0.38	98.91	9.522	6.348	0.063	2.620	1.383	0.037	0.000	0.040	20.014	64	35	1
BR4	xen	pl	core	56.04	27.25	1.09	9.98	5.54	0.50	0.13	–	100.53	10.096	5.788	0.165	1.926	1.937	0.115	0.009	0.000	20.036	48	49	3
AL2	rhy	alk feld	core	66.39	21.01	0.44	1.78	7.62	3.67	0.58	–	101.49	11.663	4.351	0.065	0.334	2.596	0.824	0.040	0.000	19.872	9	68	23
AL2	rhy	alk feld	rim	65.97	20.86	–	2.16	7.83	3.71	0.10	0.12	100.75	11.649	4.343	0.000	0.409	2.681	0.837	0.007	0.012	19.938	10	68	21
AL2	rhy	alk feld	gm	66.45	19.81	0.27	0.63	6.71	5.51	0.17	0.09	99.65	11.881	4.176	0.041	0.121	2.324	1.257	0.012	0.010	19.822	3	63	34
AL2	rhy	alk feld	gm	66.26	18.24	0.76	0.24	5.53	7.77	0.08	0.38	99.26	12.031	3.904	0.116	0.047	1.947	1.801	0.006	0.040	19.891	1	52	47
AL2	rhy	alk feld	mcr	65.71	19.09	0.41	0.31	5.71	6.96	0.98	0.80	99.97	11.902	4.075	0.062	0.061	2.007	1.608	0.070	0.084	19.868	2	55	44
AL4	rhy	alk feld	core	66.05	20.51	0.00	1.49	7.64	3.90	0.44	0.56	100.59	11.719	4.290	0.000	0.283	2.629	0.883	0.031	0.057	19.893	7	69	24
AL4	rhy	alk feld	rim	65.78	20.68	0.28	2.11	7.71	3.19	0.32	0.62	100.69	11.653	4.320	0.042	0.401	2.649	0.720	0.022	0.063	19.871	10	70	19
AL4	rhy	alk feld	core	65.44	20.30	0.68	1.51	7.70	3.46	0.51	–	99.60	11.710	4.282	0.101	0.290	2.670	0.791	0.035	0.000	19.879	8	71	22
AL4	rhy	alk feld	rim	64.64	20.98	0.64	2.28	7.72	3.07	0.20	0.47	99.99	11.547	4.417	0.096	0.436	2.674	0.699	0.014	0.048	19.931	11	70	18

(Continued)

Table 1. (Continued)

Sample	Rock name	Mineral name	Description	SiO ₂	Al ₂ O ₃	FeO	CaO	Na ₂ O	K ₂ O	BaO	SrO	Sum	Si	Al	Fe	Ca	Na	K	Ba	Sr	Sum	An	Ab	Or
AL4	rhy	alk feld	gm	65.80	20.91	0.38	1.63	7.40	3.49	0.28	0.13	100.03	11.683	4.378	0.057	0.311	2.546	0.791	0.020	0.013	19.797	8	70	22
AL4	rhy	alk feld	gm	66.75	19.46	0.45	0.48	7.82	4.58	0.61	0.56	100.70	11.875	4.082	0.067	0.091	2.697	1.040	0.043	0.058	19.952	2	70	28
AL9	rhy	alk feld	gm	63.88	17.86	0.07	0.08	0.55	16.69	-	0.16	99.29	11.971	3.946	0.012	0.016	0.200	3.990	0.000	0.017	20.151	0	5	94
AL9	rhy	alk feld	gm	64.16	17.96	0.45	0.25	0.55	16.49	-	-	99.86	11.953	3.944	0.070	0.051	0.198	3.920	0.000	0.000	20.134	1	5	94
AL9	rhy	alk feld	gm	64.39	18.52	0.17	0.29	0.61	15.62	0.08	0.27	99.96	11.929	4.044	0.026	0.058	0.219	3.692	0.006	0.029	20.004	1	6	92
AL8	rhy	alk feld	gm	66.99	19.01	0.45	-	2.87	10.83	0.27	0.43	100.85	12.042	4.028	0.068	0.000	1.000	2.485	0.019	0.045	19.687	0	29	71
AL8	rhy	alk feld	gm	64.23	18.91	1.17	0.09	0.18	16.09	-	0.24	100.91	11.843	4.111	0.180	0.018	0.063	3.784	0.000	0.025	20.025	0	2	97
AL8	rhy	alk feld	gm	64.46	18.51	--	-	0.08	15.66	0.25	0.35	99.32	11.990	4.060	0.000	0.000	0.029	3.717	0.018	0.038	19.853	0	2	98
AL8	rhy	alk feld	gm	64.48	18.13	0.18	0.21	0.13	15.72	0.75	0.34	99.94	11.993	3.976	0.029	0.043	0.046	3.730	0.054	0.036	19.907	1	2	97

pl = plagioclase; alk feld = alkali feldspar; mcr = microphenocryst; gm = groundmass. An, Ab and Or in mol.%. gph = granophyre; b.a. = basaltic andesite; xen = xenolith in BR4 sample; rhy = rhyolite. Samples BR4 (mafic) and AL4 (rhyolitic) are dykes.

with gravimetric techniques, by firing at 1000 °C small aliquots of powders previously dried at 110 °C overnight. Major and trace element (including the REE) data for the Barda–Alech rocks are presented in Table 6.

4.d. Sr–Nd isotopic analyses

Sr–Nd isotopic analyses were performed on 12 samples (six Barda granophyres, the Barda basaltic andesite dyke BR4 and five Alech rhyolitic rocks), using a fully automatic Thermo Fisher TRITON multicollector thermal ionization mass spectrometer (TIMS), located at the National Facility for Isotope Geology and Geochronology, Indian Institute of Technology Roorkee. Sample dissolution procedures and other analytical details are as described by Sheth *et al.* (2011, 2012). The Sr–Nd isotopic data are reported in Table 7.

5. Results

5.a. Mineral chemistry

Plagioclase in Barda granophyres ranges in composition from oligoclase (An₂₁₋₁₉Ab₇₂₋₇₄Or₇) to albite (An₁₁Ab₈₂Or₇). De & Bhattacharyya (1971) determined similar plagioclase phenocryst compositions of An₁₅ to An₂₁ from optic axial angle measurements. Unexsolved alkali feldspars in Barda granophyres range from An₁Ab₆₂Or₃₇ to An₁Ab₇Or₉₂ (Table 1; Fig. 5a).

In Barda basaltic andesite dyke BR4, plagioclase phenocrysts are bytownite (An₇₁₋₈₀Ab₂₇₋₂₀Or₁₋₀) whereas groundmass plagioclase ranges from labradorite (An₅₈Ab₃₉Or₃) to andesine (An₄₆₋₄₅Ab₄₉₋₅₁Or₅₋₄). Rare K-feldspar (An₁Ab₁₁Or₈₈) is found in the groundmass (Fig. 5a). Plagioclase in the basement xenoliths in dyke BR4 ranges from labradorite (An₆₄Ab₃₅Or₁) to andesine (An₅₀₋₄₈Ab₄₇₋₄₉Or₃), and the xenoliths contain rare K-feldspar (An₀Ab₆Or₉₄).

Phenocrysts of alkali feldspar in the Alech rhyolites (AL2, AL4) are anorthoclase (An₁₂₋₃Ab₇₁₋₆₃Or₁₇₋₃₄) (Table 1; Fig. 5a). Groundmass alkali feldspars range from An₂Ab₆₀Or₃₈ to An₁Ab₅₀Or₄₉. Sanidine occurs in the groundmass of Alech rhyolites AL8 and AL9 (Fig. 5a).

Pyroxenes in Barda granophyres (Table 2) are hedenbergite (Ca₄₃₋₄₆Mg₀Fe₅₇₋₅₄; Mg# = Mg*100/(Mg+Fe)_i = 0) and aegirine–augite (Na₂O = 1.8–4.6 wt %; Mg# = 0), typical of alkaline rocks (Fig. 5b). De & Bhattacharyya (1971) reported similar compositions. TiO₂ is generally low (0–0.8 wt %) and tends to decrease with decreasing FeO content of the clinopyroxene. In the basaltic andesite dyke BR4, augite (Ca₄₃₋₄₁Mg₄₁₋₄₄Fe₁₆₋₁₅; Mg# = 73–75) and orthopyroxene (Ca₂₋₃Mg₆₅₋₆₆Fe₃₁₋₃₂; Mg# = 67–69) are the two pyroxenes (Fig. 5b). Orthopyroxene with similar composition (Ca₂₋₃Mg₆₆₋₆₇Fe₃₁₋₃₂) is observed in the basement xenoliths of dyke BR4. Equilibration temperatures based on clinopyroxene–liquid geothermometer (Putirka, 2008) range from 1003 °C to 1043 °C. Two-pyroxene geothermometry (Putirka, 2008) yields values close to 900 °C.

Titaniferous magnetite in the Barda granophyres has variable TiO₂ (1.0–24.4 wt %; 3–69 mol. % ulvöspinel) and low Al₂O₃ (<0.7 wt %) contents (Table 3). In dyke BR4 the titaniferous magnetite has low ulvöspinel (11–26 mol. %) contents. Ilmenite has a limited range of solid solution with haematite (ilmenite from 85 to 95 mol. %). MgO ranges from 1.2 to 2.4 wt % in ilmenites in dyke BR4. Equilibrium magnetite–ilmenite pairs in the Barda granophyres and basaltic andesite yield temperature and log *f*O₂ of 583–750 °C and –14 to –20, respectively (calculated using the ILMAT program of Lepage, 2003), indicating late-stage subsolidus equilibration.

Table 2. Representative chemical analyses (in wt %) and structural formulas (in apfu, calculated on basis of 6 oxygens and 4 cations) of pyroxenes in the Barda rocks, Saurashtra

Sample	Rock name	Mineral name	Description	SiO ₂	TiO ₂	Al ₂ O ₃	FeO	MnO	MgO	CaO	Na ₂ O	Cr ₂ O ₃	V ₂ O ₃	Sum	Si	Ti	Al	Fe	Mn	Mg	Ca	Na	Cr	V	Sum	Mg#	Di-Hd	En-Fs	Ac	Jd
BR3	gph	cpx	mcr	47.24	0.52	0.66	29.59	1.79	-	19.95	0.98	-	0.24	100.96	1.926	0.016	0.032	1.009	0.062	0.000	0.871	0.078	0.000	0.008	4.000	0	0.86	0.08	0.08	0.00
BR3	gph	cpx	mcr	46.82	-	0.50	29.55	1.42	0.05	20.48	0.88	0.03	-	99.73	1.929	0.000	0.024	1.018	0.050	0.003	0.904	0.070	0.001	0.000	4.000	0	0.90	0.07	0.07	0.00
BR3	gph	cpx	core	46.81	0.40	0.69	30.62	1.26	0.02	19.88	1.03	0.09	-	100.80	1.911	0.012	0.033	1.045	0.044	0.001	0.869	0.082	0.003	0.000	4.000	0	0.86	0.10	0.08	0.00
BR3	gph	cpx	rim	46.52	0.63	0.50	29.31	1.68	-	20.27	1.03	0.02	-	99.98	1.913	0.020	0.024	1.008	0.059	0.000	0.893	0.082	0.001	0.000	4.000	0	0.88	0.07	0.08	0.00
BR3	gph	cpx	rim	47.38	0.28	0.42	30.08	1.50	0.14	19.78	0.79	-	0.11	100.46	1.943	0.009	0.020	1.032	0.052	0.009	0.869	0.063	0.000	0.004	4.000	1	0.86	0.09	0.06	0.00
BR3	gph	cpx	core	46.48	0.44	0.52	29.50	1.72	0.18	20.02	1.02	-	-	99.88	1.912	0.014	0.025	1.015	0.060	0.011	0.882	0.081	0.000	0.000	4.000	1	0.87	0.09	0.08	0.00
BR3	gph	cpx	rim	46.87	0.29	0.66	29.82	1.45	0.10	19.77	0.85	-	-	99.80	1.933	0.009	0.032	1.028	0.051	0.006	0.873	0.068	0.000	0.000	4.000	1	0.86	0.09	0.07	0.00
BR7	gph	cpx	mcr	47.35	0.30	0.29	30.65	0.98	0.04	19.11	1.82	0.28	-	100.83	1.920	0.009	0.014	1.039	0.034	0.002	0.830	0.143	0.009	0.000	4.000	0	0.83	0.12	0.15	0.00
BR7	gph	cpx	mcr	47.13	0.35	0.56	30.41	1.11	-	18.99	1.75	-	0.07	100.37	1.919	0.011	0.027	1.036	0.038	0.000	0.828	0.139	0.000	0.002	4.000	0	0.83	0.12	0.14	0.00
BR7	gph	cpx	mcr	47.92	0.24	0.37	30.10	1.60	0.14	17.93	2.04	0.05	-	100.41	1.946	0.007	0.018	1.022	0.055	0.009	0.780	0.161	0.002	0.000	4.000	1	0.79	0.13	0.16	0.00
BR7	gph	cpx	mcr	47.09	0.32	0.31	30.58	1.59	-	18.69	1.94	0.11	-	100.62	1.913	0.010	0.015	1.039	0.055	0.000	0.813	0.153	0.003	0.000	4.000	0	0.81	0.13	0.16	0.00
BR7	gph	cpx	mcr	47.04	0.26	0.32	30.54	1.56	0.15	18.81	1.72	0.16	0.09	100.64	1.913	0.008	0.015	1.038	0.054	0.009	0.820	0.135	0.005	0.003	4.000	1	0.82	0.13	0.14	0.00
BR7	gph	cpx	mcr	48.24	0.56	0.34	29.78	1.22	-	18.72	1.83	0.09	0.03	100.81	1.955	0.017	0.016	1.009	0.042	0.000	0.813	0.144	0.003	0.001	4.000	0	0.82	0.10	0.12	0.00
BR12	gph	cpx	mcr	48.76	0.00	0.45	29.48	2.99	0.02	15.56	3.38	0.06	-	100.69	1.955	0.000	0.021	0.988	0.101	0.001	0.668	0.262	0.002	0.000	4.000	0	0.69	0.17	0.23	0.03
BR12	gph	cpx	mcr	49.20	0.21	0.36	29.76	1.68	-	14.91	4.61	-	0.11	100.85	1.947	0.006	0.017	0.985	0.056	0.000	0.632	0.354	0.000	0.003	4.000	0	0.66	0.18	0.30	0.04
BR12	gph	cpx	mcr	49.22	0.14	0.51	30.46	0.88	-	15.01	4.36	-	-	100.58	1.955	0.004	0.024	1.012	0.029	0.000	0.639	0.336	0.000	0.000	4.000	0	0.66	0.19	0.27	0.05
BR11	gph	cpx	core	47.17	0.59	0.67	30.26	1.33	0.07	20.05	0.07	0.21	-	100.42	1.951	0.018	0.033	1.047	0.047	0.004	0.888	0.005	0.007	0.000	4.000	0	0.87	0.09	0.01	0.00
BR11	gph	cpx	core	46.84	0.60	0.43	31.63	1.02	0.17	19.61	-	-	0.40	100.69	1.938	0.019	0.021	1.094	0.036	0.010	0.869	0.000	0.000	0.013	4.000	1	0.85	0.13	0.00	0.00
BR11	gph	cpx	rim	47.02	0.28	0.75	30.50	1.08	0.15	19.49	0.29	-	0.26	99.80	1.951	0.009	0.037	1.058	0.038	0.009	0.866	0.023	0.000	0.009	4.000	1	0.85	0.11	0.02	0.00
BR11	gph	cpx	core	46.98	0.54	0.71	29.39	0.98	0.19	20.17	0.51	-	-	99.47	1.947	0.017	0.035	1.019	0.034	0.012	0.896	0.041	0.000	0.000	4.000	1	0.88	0.08	0.04	0.00
BR11	gph	cpx	core	46.89	0.66	0.39	29.79	0.97	0.18	19.99	0.17	-	-	99.03	1.962	0.021	0.019	1.042	0.034	0.011	0.896	0.014	0.000	0.000	4.000	1	0.88	0.09	0.01	0.00
BR11	gph	cpx	mcr	47.31	0.54	0.43	29.20	2.21	0.07	19.93	0.24	0.15	-	100.07	1.960	0.017	0.021	1.012	0.077	0.004	0.885	0.019	0.005	0.000	4.000	0	0.87	0.07	0.02	0.00
BR11	gph	cpx	core	47.13	0.83	0.16	30.34	1.43	0.07	18.66	0.57	0.17	-	99.36	1.967	0.026	0.008	1.059	0.051	0.004	0.834	0.046	0.006	0.000	4.000	0	0.83	0.12	0.02	0.00
BR4	b.a.	opx	gm	53.24	0.14	0.67	20.70	0.88	24.35	0.83	-	0.15	-	100.96	1.945	0.004	0.029	0.632	0.027	1.326	0.033	0.000	0.004	0.000	4.000	68	0.01	0.98	0.00	0.00
BR4	b.a.	opx	gm	52.72	0.87	0.79	20.23	0.94	23.47	1.13	-	0.23	-	100.38	1.945	0.024	0.034	0.624	0.029	1.291	0.045	0.000	0.007	0.000	4.000	67	0.02	0.95	0.00	0.00
BR4	b.a.	opx	gm	53.32	0.13	0.69	18.87	0.76	23.97	1.53	-	0.03	-	99.29	1.974	0.004	0.030	0.584	0.024	1.323	0.061	0.000	0.001	0.000	4.000	69	0.05	0.93	0.00	0.00
BR4	b.a.	opx	gm	53.05	0.13	0.85	19.77	0.58	24.38	0.87	-	0.19	-	99.81	1.954	0.004	0.037	0.609	0.018	1.339	0.034	0.000	0.005	0.000	4.000	69	0.02	0.97	0.00	0.00
BR4	b.a.	opx	gm	53.27	0.19	0.50	20.57	0.68	24.38	0.80	-	-	0.15	100.55	1.953	0.005	0.022	0.631	0.021	1.333	0.031	0.000	0.000	0.004	4.000	68	0.01	0.98	0.00	0.00
BR4	b.a.	opx	gm	53.73	0.09	0.64	19.67	0.63	23.87	1.22	-	-	0.23	100.09	1.979	0.002	0.028	0.606	0.020	1.311	0.048	0.000	0.000	0.007	4.000	68	0.03	0.94	0.00	0.00
BR4	b.a.	cpx	gm	54.36	0.50	0.87	8.60	0.25	14.60	20.33	0.19	-	-	99.71	2.030	0.014	0.038	0.269	0.008	0.813	0.814	0.014	0.000	0.000	4.000	75	0.77	0.15	0.00	0.01

(Continued)

Table 2. (Continued)

Rock name	Mineral name	Description	SiO ₂	TiO ₂	Al ₂ O ₃	FeO	MnO	MgO	CaO	Na ₂ O	Cr ₂ O ₃	V ₂ O ₅	Sum	Si	Ti	Al	Fe	Mn	Mg	Ca	Na	Cr	V	Sum	Mg#	Di-	En-	Ac	Jd	
BR4	b.a.	cpx	gm	52.77	0.27	0.95	8.78	0.51	14.87	20.92	0.09	-	0.23	99.39	1.976	0.008	0.042	0.275	0.016	0.830	0.839	0.006	0.000	0.007	4.000	75	0.82	0.14	0.00	0.01
BR4	b.a.	cpx	gm	52.78	0.31	1.03	9.11	0.55	15.64	20.34	0.03	0.10	-	99.89	1.963	0.009	0.045	0.283	0.017	0.867	0.811	0.002	0.003	0.000	4.000	75	0.79	0.18	0.00	0.00
BR4	b.a.	cpx	mcr	52.70	0.35	1.12	9.49	0.54	14.40	21.05	-	-	-	99.64	1.976	0.010	0.049	0.297	0.017	0.805	0.845	0.000	0.000	0.000	4.000	73	0.82	0.14	0.00	0.00
BR4	b.a.	cpx	gm	53.03	0.47	0.89	8.70	0.34	15.01	21.29	0.06	0.08	-	99.85	1.976	0.013	0.039	0.271	0.011	0.834	0.850	0.005	0.002	0.000	4.000	75	0.83	0.14	0.00	0.00
BR4	xen	opx	core	53.31	-	0.73	19.54	0.55	24.26	1.44	-	-	0.12	99.95	1.960	0.000	0.032	0.601	0.017	1.330	0.057	0.000	0.000	0.003	4.000	69	0.04	0.95	0.00	0.00
BR4	xen	opx	core	52.87	0.17	1.07	19.49	0.42	24.14	1.24	-	-	0.18	99.57	1.951	0.005	0.047	0.602	0.013	1.329	0.049	0.000	0.000	0.005	4.000	69	0.03	0.96	0.00	0.00
BR4	xen	opx	core	53.51	0.33	0.79	19.20	0.62	24.36	1.07	-	-	0.08	99.96	1.967	0.009	0.034	0.590	0.019	1.335	0.042	0.000	0.000	0.002	4.000	69	0.02	0.95	0.00	0.00

gph = granophyre; b.a. = basaltic andesite; xen = xenolith in BR4 sample. mcr = microphenocryst; gm = groundmass; opx = orthopyroxene; cpx = clinopyroxene. Mg# = atomic 100*(Mg+Fe). Pyroxene components: Di-Hd = diopside-hedenbergite; En-Fs = enstatite-ferrosilite; Ac = acmite; Jd = jadeite.

Zircon and titanite are ubiquitous in the Barda granophyres as euhedral, prismatic microcrystals and show a homogeneous major element composition. Zircon contains up to 2.4 wt % HfO₂ (Table 4). Monazite-(Ce) has been observed as accessory phase in the Alech rhyolite AL9. It contains La₂O₃ in the range 15.1–20.3 wt % and Ce₂O₃ from 34.0 to 42.6 wt %. Thorium concentration ranges from 1.1 to 7.4 wt % ThO₂ (Table 4).

5.b. ⁴⁰Ar-³⁹Ar dating

Granophyre BR3 yielded an 11-step plateau constituting as much as 89.4 % of the total ³⁹Ar release, and an age of 68.5 ± 0.4 Ma (2σ) (Fig. 6a). Granophyre BR5 yielded a 12-step plateau constituting 81.3 % of the ³⁹Ar release, and an age of 69.9 ± 0.3 (2σ) (Fig. 6b). Granophyre BR12 yielded a seven-step plateau constituting 67.1 % of the ³⁹Ar release, and an age of 69.0 ± 0.5 (2σ) (Fig. 6c). All three samples have isochron ages and inverse isochron ages that are statistically indistinguishable from the plateau ages (Fig. 6a–c; Table 5). The isochrons and inverse isochrons also have acceptable MSWD values and intercepts showing atmospheric values (295.5) of the trapped ⁴⁰Ar/³⁶Ar ratio, which suggests, along with the well-developed plateau spectra for all samples, that these ages are true crystallization ages. We take the plateau ages of the three granophyre samples to represent their intrusion and crystallization ages.

5.c. Whole-rock geochemistry

5.c.1. Alteration effects

Like hand specimen and petrographic observations, LOI values indicate that several samples (particularly of the Alech rocks, e.g. AL3, 5, 10, 11) are altered. LOI values range from 0.30 to 1.64 wt % for Barda rock samples and from 1.10 to 5.51 wt % for Alech rock samples. The extremely high SiO₂ content in some Alech rhyolites (e.g. 86.71 wt % in AL3) indicates silicification processes mostly associated with alkali mobility. Alteration also appears to have variably affected K, Na, Rb and Ba contents in the Alech samples, as noted from poor correlations between K, Na, Rb and Ba and more alteration-resistant elements such as Zr or Nb. We therefore do not use Rb, Ba, K and Na data in this study and use only the alteration-resistant elements (Ti, Zr, Nb, Y, Th and REE) and their ratios for geochemical interpretations.

5.c.2. Major- and trace-element compositions

We used the SINCLAS program of Verma *et al.* (2002) to recalculate the major oxide data on an LOI-free basis and to obtain rock names recommended by the IUGS Sub-commission on the Systematics of Igneous Rocks based on the total alkalis-silica diagram (Le Bas *et al.* 1986). As given by SINCLAS, all Barda granophyres are of rhyolite composition, whereas the dyke BR4 is a basaltic andesite. Most Alech samples are also of rhyolite composition, including dyke AL4, but sample AL07 from the outcrop with flow folding (Fig. 3b) and dyke AL11 from Chek Hill are dacites. The basaltic andesite dyke BR4 has 7 wt % normative quartz (Supplementary Table S2, available online at <https://doi.org/10.1017/S0016756818000924>).

The Barda granophyres are mainly metaluminous (A/CNK = mol Al₂O₃/(CaO+Na₂O+K₂O) = 0.88–0.93). They are chemically uniform, with SiO₂ in the range 70.2–72.9 wt %, TiO₂ 0.3–0.5 wt %, Al₂O₃ 11.6–12.7 wt % and Fe₂O_{3t} 4.4–5.8 wt %. All samples contain very low MgO contents (0.1–0.2 wt %). The alteration-resistant trace elements also have narrow ranges of concentration (Zr = 447–557 ppm, Nb = 49–55 ppm, Y = 87–112 ppm) and ratios

Table 3. Representative chemical analyses (in wt %) and structural formulas (in apfu) of magnetites and ilmenites in the Barda rocks, Saurashtra

Sample	Rock name	Mineral name	Description	TiO ₂	Al ₂ O ₃	Fe ₂ O ₃	FeO	MnO	MgO	Cr ₂ O ₃	V ₂ O ₃	NiO	Sum	Ti	Al	Fe ³⁺	Fe ²⁺	Mn	Mg	Cr	V	Ni	Sum	Ulv	Ilm
BR3	gph	mgt	core	6.85	0.64	54.65	36.83	0.57	–	–	0.11	0.11	99.75	0.197	0.029	1.572	1.178	0.018	0.000	0.000	0.003	0.003	3.001	20	–
BR3	gph	mgt	core	16.85	0.43	35.58	44.93	1.79	–	0.10	0.14	–	99.82	0.480	0.019	1.014	1.423	0.057	0.000	0.003	0.004	0.000	3.000	48	–
BR3	gph	mgt	core	12.03	0.29	45.66	41.45	0.90	0.02	–	0.03	0.09	100.47	0.342	0.013	1.300	1.312	0.029	0.001	0.000	0.001	0.003	3.001	34	–
BR3	gph	mgt	core	1.65	0.41	64.93	32.31	0.18	–	–	0.06	–	99.53	0.048	0.019	1.884	1.042	0.006	0.000	0.000	0.002	0.000	3.000	5	–
BR5	gph	mgt	core	0.95	0.05	67.65	31.99	0.20	–	–	–	–	100.84	0.027	0.002	1.943	1.021	0.006	0.000	0.000	0.000	0.000	3.000	3	–
BR5	gph	mgt	core	1.27	0.30	65.86	31.47	0.68	–	–	0.05	0.52	100.16	0.037	0.014	1.903	1.011	0.022	0.000	0.000	0.002	0.016	3.004	4	–
BR5	gph	mgt	core	1.25	0.11	66.68	31.77	0.33	0.15	–	0.09	–	100.38	0.036	0.005	1.920	1.017	0.011	0.008	0.000	0.003	0.000	3.000	4	–
BR5	gph	mgt	core	0.95	0.04	66.59	31.15	0.27	0.21	–	0.18	–	99.39	0.028	0.002	1.937	1.007	0.009	0.012	0.000	0.006	0.000	3.000	3	–
BR7	gph	mgt	core	10.06	0.20	49.04	38.21	2.12	–	–	0.10	0.26	99.98	0.289	0.009	1.407	1.218	0.068	0.000	0.000	0.003	0.008	3.002	28	–
BR7	gph	mgt	core	13.29	0.42	42.92	42.34	1.21	–	0.04	0.06	0.27	100.57	0.377	0.019	1.219	1.337	0.039	0.000	0.001	0.002	0.008	3.002	38	–
BR12	gph	mgt	core	24.37	0.19	21.92	52.84	1.15	–	–	0.36	–	100.81	0.683	0.008	0.615	1.647	0.036	0.000	0.000	0.011	0.000	3.000	69	–
BR4	b.a.	mgt	core	4.44	1.15	57.75	34.33	0.09	0.61	0.99	0.54	0.11	100.01	0.127	0.051	1.648	1.088	0.003	0.035	0.030	0.016	0.003	3.001	13	–
BR4	b.a.	mgt	core	3.67	1.25	58.80	33.61	0.29	0.49	1.53	0.23	–	99.87	0.105	0.056	1.681	1.068	0.009	0.028	0.046	0.007	0.000	3.000	11	–
BR5	gph	ilm	mcr	49.68	–	4.59	36.56	8.03	–	–	0.76	–	99.62	0.948	0.000	0.088	0.776	0.173	0.000	0.000	0.015	0.000	2.000	–	95
BR5	gph	ilm	mcr	48.26	0.10	8.51	33.37	9.91	–	–	0.65	–	100.80	0.912	0.003	0.161	0.701	0.211	0.000	0.000	0.013	0.000	2.000	–	91
BR5	gph	ilm	mcr	47.58	–	8.80	34.81	7.89	–	0.47	0.04	–	99.59	0.911	0.000	0.168	0.741	0.170	0.000	0.009	0.001	0.000	2.000	–	91
BR7	gph	ilm	incl	49.55	0.25	6.37	41.56	2.93	0.02	0.10	0.07	–	100.85	0.935	0.007	0.120	0.871	0.062	0.001	0.002	0.001	0.000	2.000	–	94
BR4	b.a.	ilm	gm	46.38	0.28	12.55	37.40	0.72	2.02	–	0.43	–	99.78	0.873	0.008	0.236	0.783	0.015	0.075	0.000	0.009	0.000	2.000	–	87
BR4	b.a.	ilm	gm	44.82	0.10	14.83	34.97	0.98	2.45	–	0.88	0.62	99.65	0.846	0.003	0.280	0.733	0.021	0.091	0.000	0.018	0.013	2.004	–	85
BR4	b.a.	ilm	gm	46.46	0.15	11.83	37.84	1.73	1.23	–	0.40	–	99.64	0.881	0.005	0.225	0.798	0.037	0.046	0.000	0.008	0.000	2.000	–	88
BR4	b.a.	ilm	gm	46.44	0.04	12.40	37.91	1.36	1.40	–	0.18	0.23	99.96	0.879	0.001	0.235	0.797	0.029	0.052	0.000	0.004	0.005	2.002	–	88

gph = granophyre; b.a. = basaltic andesite; gm = groundmass; incl = inclusion; mcr = microphenocryst; mgt = magnetite; ilm = ilmenite. Ulv = ulvöspinel mol. %; Ilm = ilmenite mol. % magnetites were calculated on the basis of 4 oxygens and 3 cations; ilmenites were calculated on the basis of 3 oxygens and 2 cations.

Table 4. Representative chemical analyses (in wt %) and structural formulas (in apfu) of zircons, titanites, apatites and monazites in the Barda–Alech rocks, Saurashtra

Sample	BR3	BR3	BR7	BR7	BR5	BR5	BR5	BR7	AL2	AL2	AL9	AL9
Rock name	gph	gph	gph	gph	gph	gph	gph	gph	rhy	rhy	rhy	rhy
Mineral name	zircon	zircon	zircon	zircon	titanite	titanite	titanite	titanite	apatite	apatite	monazite	monazite
Description	incl	incl	mcr	mcr	mcr	mcr	mcr	mcr	incl	incl	gm	gm
SiO ₂	32.33	31.83	31.43	32.08	30.92	29.71	29.79	28.89	0.28	0.83	2.08	1.52
TiO ₂	–	–	–	–	29.06	30.24	38.25	28.75	–	–	–	–
Al ₂ O ₃	–	–	–	–	4.07	0.84	0.16	0.60	–	–	–	–
FeO	–	0.26	0.13	–	5.29	4.98	1.61	6.05	0.90	0.77	–	0.60
CaO	–	–	–	–	28.04	25.63	28.23	26.14	55.19	55.06	0.61	0.21
Na ₂ O	–	–	–	–	0.49	0.67	0.54	0.80	–	–	–	–
P ₂ O ₅	–	–	–	–	–	–	–	–	41.63	41.18	27.79	27.88
SrO	–	–	–	–	0.24	–	0.04	–	1.30	1.14	0.67	0.46
ZrO ₂	66.74	65.86	65.42	65.79	–	0.27	0.27	–	–	–	–	–
Nb ₂ O ₅	–	–	–	–	0.07	2.28	0.70	3.74	–	–	–	–
La ₂ O ₃	–	–	–	–	0.27	0.89	0.42	1.91	–	–	20.28	15.05
Ce ₂ O ₃	–	–	–	–	0.13	0.42	0.16	1.37	–	–	33.99	42.61
Nd ₂ O ₃	–	–	–	–	–	1.25	0.13	0.72	–	–	4.47	9.47
HfO ₂	0.12	1.55	1.92	2.38	–	–	–	–	–	–	–	–
ThO ₂	–	–	–	–	–	–	–	–	–	–	7.39	1.16
F	–	–	–	–	–	–	–	–	1.08	–	–	–
Cl	–	–	–	–	–	–	–	–	0.07	–	–	0.02
SO ₃	–	–	–	–	–	–	–	–	0.58	0.26	0.13	0.04
Sum	99.20	99.50	98.90	100.25	98.58	97.20	100.31	98.95	99.31	98.99	97.27	98.95
O=F,Cl	–	–	–	–	–	–	–	–	0.47	–	–	0.01
Sum	99.20	99.50	98.9	100.25	98.58	97.20	100.31	98.95	100.57	99.24	97.40	99.01
Si	0.996	0.987	0.983	0.990	1.044	1.040	0.986	1.015	0.045	0.132	0.083	0.060
Ti	0.000	0.000	0.000	0.000	0.738	0.796	0.953	0.760	0.000	0.000	0.000	0.000
Al	0.000	0.000	0.000	0.000	0.162	0.035	0.006	0.025	0.000	0.000	0.000	0.000
Fe	0.000	0.007	0.003	0.000	0.149	0.146	0.045	0.178	0.120	0.104	0.000	0.020
Ca	0.000	0.000	0.000	0.000	1.014	0.961	1.001	0.984	9.422	9.458	0.026	0.009
Na	0.000	0.000	0.000	0.000	0.032	0.045	0.035	0.054	0.000	0.000	0.000	0.000
P	0.000	0.000	0.000	0.000	0.000	0.000	0.000	0.000	5.616	5.590	0.942	0.940
Sr	0.000	0.000	0.000	0.000	0.005	0.000	0.001	0.000	0.120	0.106	0.015	0.011
Zr	1.003	0.996	0.998	0.989	0.000	0.005	0.004	0.000	0.000	0.000	0.000	0.000
Nb	0.000	0.000	0.000	0.000	0.001	0.036	0.010	0.059	0.000	0.000	0.000	0.000
La	0.000	0.000	0.000	0.000	0.003	0.012	0.005	0.025	0.000	0.000	0.299	0.221
Ce	0.000	0.000	0.000	0.000	0.002	0.005	0.002	0.018	0.000	0.000	0.498	0.621
Nd	0.000	0.000	0.000	0.000	0.000	0.016	0.002	0.009	0.000	0.000	0.064	0.135
Hf	0.001	0.014	0.017	0.021	0.000	0.000	0.000	0.000	0.000	0.000	0.000	0.000
Th	0.000	0.000	0.000	0.000	0.000	0.000	0.000	0.000	0.000	0.000	0.067	0.010
S	0.000	0.000	0.000	0.000	0.000	0.000	0.000	0.000	0.070	0.031	0.004	0.001
Sum	2.000	2.003	2.002	2.000	3.150	3.095	3.050	3.126	15.392	15.421	1.999	2.028

gph = granophyre; rhy = rhyolite; mcr = microphenocryst; gm = groundmass.

zircons were calculated on the basis of 4 oxygens and 2 cations; titanites were calculated on the basis of 5 oxygens and 3 cations.

apatites were calculated on the basis of 24 oxygens and 16 cations; monazites were calculated on the basis of 4 oxygens and 2 cations.

Table 5. Summary of ^{40}Ar - ^{39}Ar dating results for granophyres of the Barda complex, Saurashtra

Sample	Plateau steps	% ^{39}Ar	Age (Ma)	MSWD	p	Isochron				Inverse isochron			
						Age (Ma)	Trap	MSWD	p	Age (Ma)	Trap	MSWD	p
BR3	11	89.4	68.5 ± 0.4	0.85	0.58	68.5 ± 0.6	295.9 ± 2.2	0.31	0.97	68.5 ± 0.5	296.0 ± 1.6	0.78	0.64
BR5	12	81.3	69.9 ± 0.3	0.41	0.95	69.8 ± 0.6	296.6 ± 3.9	0.12	1.00	69.8 ± 0.5	297.0 ± 2.7	0.21	1.00
BR7	7	67.1	69.0 ± 0.5	0.18	0.98	69.0 ± 0.9	295.4 ± 3.8	0.13	0.98	68.9 ± 0.7	295.7 ± 2.8	0.23	0.95

Notes: Trap is initial $^{40}\text{Ar}/^{39}\text{Ar}$ ratio (trapped component), MSWD is mean square weighted deviate and p is the corresponding probability. Errors are reported at the 2σ confidence level and monitor mineral is MMHb (523.1 ± 2.6 Ma, Renne *et al.* 1998).

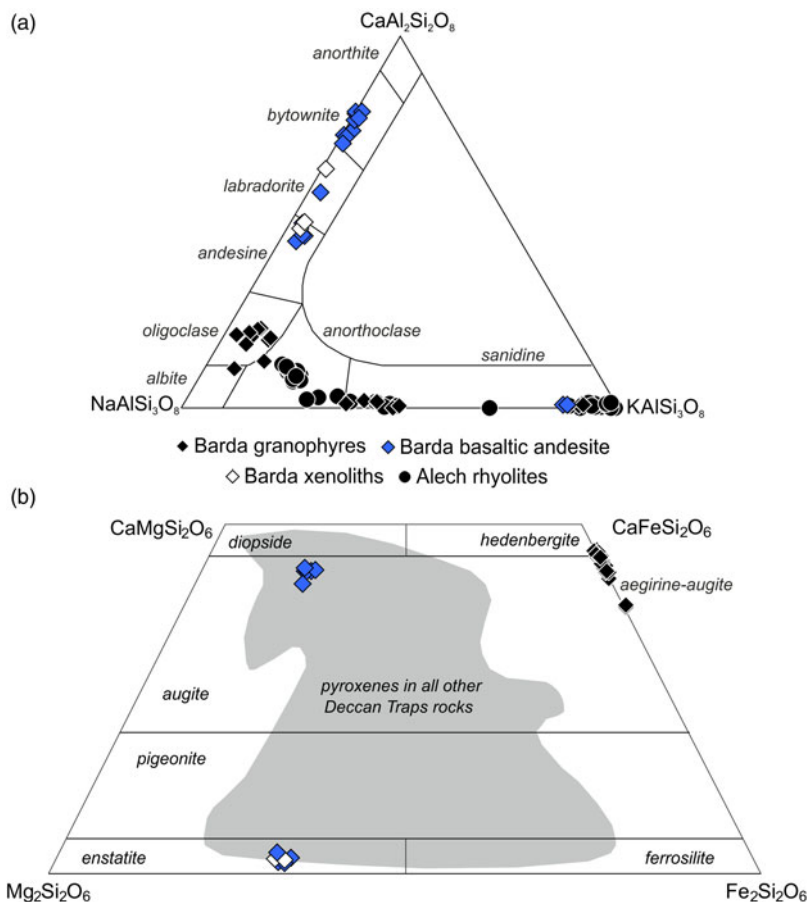


Fig. 5. (Colour online) Mineral compositions. (a) Feldspar compositions observed in the Barda and Alech rocks. (b) Pyroxene compositions of Barda–Alech rocks projected in the Ca–Mg–Fe quadrilateral. Grey shaded field contains pyroxene analyses for all analysed Deccan rocks taken together (Cucciniello *et al.* 2015 and references therein).

of concentrations ($\text{Zr}/\text{Nb} = 9\text{--}10$, $\text{Y}/\text{Nb} = 1.7\text{--}2.3$). The values of these ratios are not too different from those of mantle-derived mafic melts with slightly enriched composition and are similar to those of various Deccan (particularly Saurashtra) mafic lavas and dykes ($\text{Zr}/\text{Nb} = 5\text{--}26$; $\text{Y}/\text{Nb} = 1\text{--}9$; Cucciniello *et al.* 2015 and references therein).

The Barda granophyres show low to moderate light- to heavy REE fractionation in chondrite-normalized patterns ($\text{La}_n/\text{Yb}_n = 2.7\text{--}4.5$; the subscript 'n' means chondrite-normalized; Fig. 7a). All granophyres show distinct negative Eu anomalies, with $\text{Eu}_n/\text{Eu}^* = 0.5\text{--}0.7$, where $\text{Eu}^* = (\text{Sm}_n + \text{Gd}_n)/2$. Basaltic andesite BR4 has lower REE contents than the granophyres and has a small negative Eu anomaly ($\text{Eu}_n/\text{Eu}^* = 0.8$) in its chondrite-normalized REE pattern (Fig. 7a). In primitive mantle-normalized multi-element patterns (Fig. 7b) the Barda

granophyres show small or no troughs at Nb and marked troughs at Sr and Ti. The basaltic andesite BR4 shows negative Nb, Sr and Ti anomalies in its pattern.

The least altered (LOI < 3.4 wt %) of the Alech rhyolites and dacites (samples AL1, 4, 7, 8, 9, with $\text{SiO}_2 = 66.5\text{--}72.6$ wt %) are weakly peraluminous, with $\text{A}/\text{CNK} = 0.98\text{--}1.14$, and low (0.3 wt %) or no corundum in the CIPW norm (Supplementary Table S2, available online at <https://doi.org/10.1017/S0016756818000924>). They can be divided into two groups. The first group (samples AL5, 7, 8, 10, 11) is characterized by low Nb (20–27 ppm) and moderate Zr (282–384 ppm) and Y (43–73 ppm) contents. These rocks are slightly enriched in light REE (LREE), with La_n/Yb_n ranging from 3.7 to 4.1. Their REE patterns are relatively flat in the middle and heavy REE (HREE) portions of the pattern (Fig. 8a), with $\text{Gd}_n/\text{Lu}_n \approx 0.8\text{--}1.0$. Negative Eu anomalies ($\text{Eu}_n/\text{Eu}^* = 0.6\text{--}0.7$) are

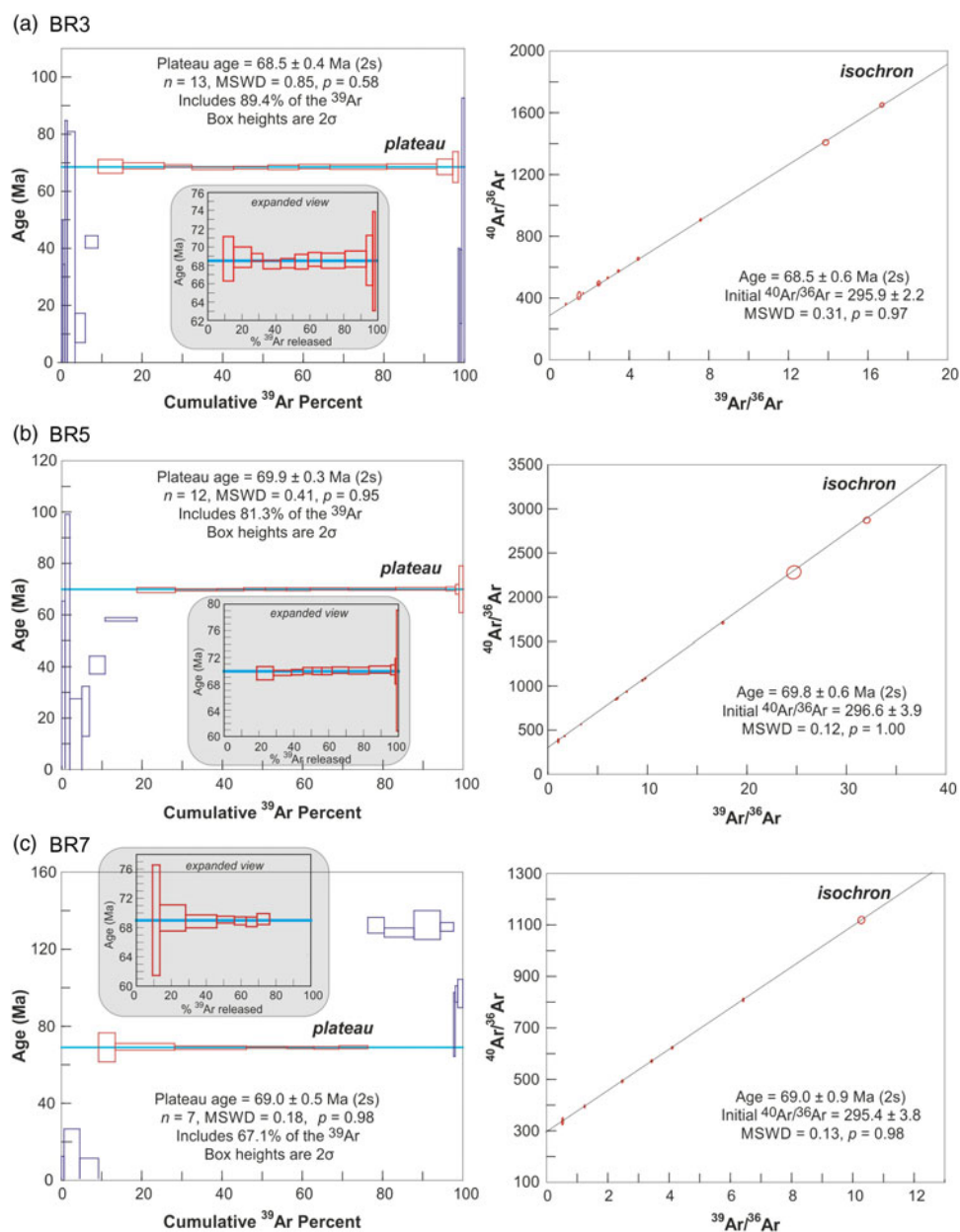


Fig. 6. (Colour online) ^{40}Ar - ^{39}Ar plateau spectra (left panels) and isochron plots (right panels) for the Barda granophyre samples (a) BR3, (b) BR5 and (c) BR7. In the plateau spectra, the plateau steps are shown with red outlines and the non-plateau steps with dark blue outlines. Also shown are values of the MSWD (mean square weighted deviate) and probability (p). Inset figures show the enlarged views of the plateau spectra.

present in the chondrite-normalized REE patterns of this group, and their mantle-normalized incompatible element patterns display troughs at Nb, Sr and Ti (Fig. 8a). The second group (samples AL1, 3, 4, 9) shows significant enrichments in the incompatible elements compared to the first group, with high Nb (108–852 ppm), Zr (584–2650 ppm) and Y (89–291 ppm) concentrations. Their chondrite-normalized patterns are characterized by moderate enrichment in LREE ($\text{La}_n/\text{Yb}_n = 4.3$ – 5.7), a very flat HREE pattern and negative Eu anomalies, with the lowest value of Eu_n/Eu^* (0.04) found in the rhyolite AL09 (Fig. 8b). In their mantle-normalized multi-element patterns (Fig. 8b), this group shows troughs at Sr and Ti.

Samples AL8 and AL9 were taken from adjacent rhyolite dykes just south of Dhoriyo Nes hamlet (Fig. 2). At Dhoriyo Nes, Maithani *et al.* (1996) have described a few rhyolite dykes with strong enrichments in Nb (up to 1000 ppm), Zr (>1000 ppm) and Y (up to 337 ppm). Our dyke AL9 (852 ppm Nb, 2650 ppm Zr, 291 ppm Y) undoubtedly represents one of them. The associated dyke AL8 does not show these notable Nb–Zr–Y enrichments.

5.c.3. Sr–Nd isotopic compositions

Measured Sr–Nd isotopic ratios of the 12 analysed Barda–Alech rocks have been recalculated as initial ratios at 65 Ma (Table 7; Fig. 9). Six Barda granophyres show a restricted range of $(^{87}\text{Sr}/^{86}\text{Sr})_t$ from 0.705987 to 0.706176. Their $(^{143}\text{Nd}/^{144}\text{Nd})_t$ values range from 0.512555 ($\epsilon_{\text{Nd}t} = 0.0$) to 0.512614 ($\epsilon_{\text{Nd}t} = +1.1$). The Barda basaltic andesite dyke BR4 has the highest $(^{87}\text{Sr}/^{86}\text{Sr})_t$ of 0.707392 and lowest $(^{143}\text{Nd}/^{144}\text{Nd})_t$ of 0.510996 ($\epsilon_{\text{Nd}t} = -30.4$) of all the analysed samples. Alech rocks of the first group described above (here represented by samples AL5, 7, 10, 11) have higher radiogenic $(^{87}\text{Sr}/^{86}\text{Sr})_t$ ratios (0.706361–0.707379), and lower radiogenic $(^{143}\text{Nd}/^{144}\text{Nd})_t$ ratios (0.512485–0.512517, $\epsilon_{\text{Nd}t} = -1.4$ to -0.7), compared to those of the second group (here represented by a single sample AL4) which has $(^{87}\text{Sr}/^{86}\text{Sr})_t = 0.705894$ and $(^{143}\text{Nd}/^{144}\text{Nd})_t = 0.512655$; $\epsilon_{\text{Nd}t} = +2.0$) and the Barda granophyres (Fig. 9).

Samples AL10 and AL11 have identical $(^{87}\text{Sr}/^{86}\text{Sr})_t$ and $(^{143}\text{Nd}/^{144}\text{Nd})_t$ ratios (Table 6; Fig. 9). AL10 is a tuffaceous-looking

Table 6. Major and trace element data for rocks of the Barda and Alech complexes, Saurashtra

Sample	BR1	BR3	BR4	BR5	BR7	BR11	BR12	AL1	AL3	AL4	AL5	AL7	AL8	AL9	AL10	AL11	W-2a Meas	W-2a Cert	SY-4 Meas	SY-4 Cert	JR-1 Meas	JR-1 Cert
Rock type	gph	gph	b.a.	gph	gph	gph	gph	rhy	rhy	rhy	rhy	dac	rhy	rhy	rhy	dac						
SiO ₂	70.21	72.92	52.97	72.44	73.04	72.46	71.27	69.82	86.71	71.29	77.28	66.53	69.35	72.56	77.72	65.60	52.48	52.40	49.71	49.90	-	-
TiO ₂	0.47	0.35	1.12	0.31	0.29	0.30	0.35	0.35	0.24	0.34	1.02	0.78	0.57	0.23	0.73	1.12	1.06	1.06	0.29	0.29	-	-
Al ₂ O ₃	12.73	11.94	16.99	11.82	11.56	11.82	11.85	13.97	7.03	13.30	12.88	12.24	12.97	11.44	10.43	11.42	15.55	15.40	20.35	20.69	-	-
Fe ₂ O _{3t}	5.84	4.71	13.52	4.91	4.35	4.45	5.67	3.63	1.03	4.43	1.85	8.87	4.99	5.32	4.40	11.47	10.77	10.70	6.06	6.21	-	-
MnO	0.05	0.09	0.15	0.12	0.07	0.08	0.12	0.03	0.01	0.09	0.05	0.16	0.03	0.04	0.01	0.12	0.17	0.16	0.11	0.11	-	-
MgO	0.16	0.04	4.06	0.07	0.06	0.05	0.08	0.13	0.03	0.07	0.08	0.21	0.61	0.03	0.11	0.22	6.25	6.37	0.51	0.54	-	-
CaO	0.59	1.17	7.23	0.31	1.05	0.92	1.48	0.21	0.22	0.36	0.28	1.96	1.06	0.63	0.13	0.38	11.03	10.90	8.14	8.05	-	-
Na ₂ O	4.11	4.02	2.56	4.03	3.96	4.03	4.18	3.91	0.03	4.39	0.06	2.94	3.11	3.66	0.03	0.75	2.23	2.14	6.96	7.10	-	-
K ₂ O	3.83	3.86	0.83	3.80	3.99	3.99	3.55	4.96	0.11	4.77	1.04	3.26	4.31	4.15	0.55	4.29	0.62	0.63	1.66	1.66	-	-
P ₂ O ₅	0.05	0.01	0.04	0.01	0.01	0.01	0.01	0.01	0.02	0.02	0.04	0.20	0.09	0.01	0.15	0.21	0.13	0.13	0.13	0.13	-	-
LOI	1.64	0.41	0.30	1.09	0.86	0.41	1.27	2.06	3.44	1.01	5.51	3.26	2.85	1.47	4.94	4.83	-	-	-	-	-	-
Total	99.69	99.52	99.76	98.90	99.24	98.52	99.82	99.08	98.87	100.07	100.08	100.41	99.94	99.54	99.20	100.42	100.29	99.89	93.91	94.68	-	-
Be	2	3	1	3	3	3	3	3	2	4	2	2	2	14	1	< 1	< 1	1.3	3	2.6	-	-
V	6	< 5	253	7	< 5	< 5	5	5	13	5	10	9	34	8	22	51	266	262	9	8	-	-
Cr	710	630	420	920	930	860	810	430	540	800	100	320	390	490	500	100	90	92	-	-	-	-
Co	2	1	40	2	2	2	2	1	1	2	3	8	4	1	8	22	43	43	-	-	-	-
Ni	20	30	100	< 20	30	50	20	< 20	30	30	< 20	< 20	< 20	< 20	20	< 20	80	70	-	-	< 20	1.67
Cu	560	1190	2070	360	810	2550	610	750	1080	1200	120	450	640	520	540	330	110	110	-	-	< 10	2.68
Zn	450	850	1250	300	670	1440	470	610	750	810	90	360	450	520	260	220	80	80	-	-	30	30.6
Ga	21	21	19	20	20	21	20	24	19	23	20	19	18	34	18	18	18	17	-	-	15	16.1
Ge	1	2	2	1	2	2	2	1	2	2	1	2	1	2	2	1	2	1	-	-	2	1.88
As	< 5	< 5	< 5	< 5	< 5	< 5	< 5	< 5	< 5	< 5	< 5	< 5	< 5	< 5	< 5	< 5	< 5	1.2	-	-	15	16.3
Rb	122	123	36	117	127	126	104	143	5	145	23	78	101	377	20	87	20	21	-	-	252	257
Sr	84	65	135	62	65	52	69	43	67	59	18	77	72	18	191	157	200	190	1194	1191	-	-
Y	112	108	24	87	103	102	102	109	89	106	73	63	67	291	53	43	20	24	117	119	-	-
Zr	447	557	123	454	523	525	495	610	647	584	357	336	384	2650	300	282	95	94	538	517	-	-
Nb	49	55	5	50	52	53	55	108	123	108	27	26	26	852	20	21	-	-	-	-	15	15.2
Mo	6	6	2	6	7	7	7	4	18	8	< 2	3	3	7	6	2	< 2	0.6	-	-	3	3.25
Sn	17	28	42	11	22	56	16	21	29	29	5	11	15	39	9	6	-	-	-	-	3	2.86
Cs	1.6	2.1	1.3	1.7	2.1	2	1.7	0.9	< 0.5	1.4	< 0.5	1.5	1.5	2.7	< 0.5	0.6	-	-	-	-	20.6	20.8
Ba	921	951	244	1034	895	944	915	1259	132	1782	385	833	1059	85	471	1481	173	182	348	340	-	-

(Continued)

Table 6. (Continued)

Sample	BR1	BR3	BR4	BR5	BR7	BR11	BR12	AL1	AL3	AL4	AL5	AL7	AL8	AL9	AL10	AL11	W-2a Meas	W-2a Cert	SY-4 Meas	SY-4 Cert	JR-1 Meas	JR-1 Cert
La	83.6	66.5	14.1	50.4	63.5	64.6	61.1	119	93	84.2	48.5	42.7	45.1	254	39.2	35.7	10.1	10	-	-	19	19.7
Ce	126	130	31.9	117	124	128	120	146	170	153	95.1	85.6	88.5	475	77.2	71.5	24.3	23	-	-	44.9	47.2
Pr	16.9	14.3	3.64	11.6	13.5	13.9	13.3	23.6	18.3	16.5	10.9	9.62	10.2	48.4	9.36	7.96	-	-	-	-	5.6	5.58
Nd	64.2	54.2	15.3	44.1	50.1	53.5	51.3	86.6	64	61.7	42.9	37	38.3	160	35.7	30.1	13.2	13	-	-	21.9	23.3
Sm	13.9	12.5	4.1	10.3	11.5	12.1	11.4	17.7	11.4	12.5	9.6	8.2	8.8	32.8	7.6	6.3	3.4	3.3	-	-	5.5	6.03
Eu	3.17	2.31	1.16	2.60	1.94	2.19	2.65	3.62	0.71	2.72	2.30	2.07	1.84	0.44	1.88	1.56	-	-	-	-	0.27	0.3
Gd	15.60	14.10	4.60	11.50	13.00	13.50	13.10	18.00	10.60	13.80	10.20	9.10	9.50	33.90	8.00	6.30	-	-	-	-	5.5	5.06
Tb	2.80	2.70	0.80	2.20	2.40	2.60	2.50	3.00	2.10	2.50	1.80	1.60	1.60	6.60	1.30	1.10	0.6	0.63	-	-	1.1	1.01
Dy	18.50	18.70	5.10	15.80	17.10	17.80	17.00	19.80	14.80	17.00	12.40	11.10	11.20	45.70	8.90	7.60	-	-	-	-	6	5.69
Ho	4.10	4.10	1.10	3.50	3.80	4.00	3.70	4.10	3.40	3.80	2.70	2.40	2.40	10.10	2.00	1.80	0.8	0.76	-	-	-	-
Er	12.40	12.80	3.00	11.20	11.70	12.20	11.60	12.60	10.50	11.90	8.00	7.20	7.30	31.80	6.00	5.50	-	-	-	-	-	-
Tm	1.89	1.99	0.45	1.76	1.84	1.92	1.79	1.97	1.64	1.88	1.22	1.11	1.12	5.02	0.97	0.86	-	-	-	-	0.62	0.67
Yb	12.50	13.40	3.00	12.40	12.70	13.00	12.80	14.10	11.20	13.10	8.60	7.70	7.90	33.80	6.50	5.90	2.1	2.1	-	-	4.6	4.55
Lu	1.93	2.06	0.48	1.95	1.96	2.01	2.02	2.37	1.75	2.17	1.38	1.25	1.26	5.13	1.02	0.95	0.31	0.33	-	-	0.7	0.71
Hf	10.0	12.4	3.0	10.1	11.7	11.7	10.8	13.2	13.7	12.5	8.0	7.7	8.8	59.2	6.1	6.1	-	-	-	-	4.4	4.51
Ta	3.8	4.4	0.4	4.0	4.4	4.2	4.2	8.8	11.6	8.3	1.9	1.8	1.9	72.1	1.5	1.5	0.5	0.5	-	-	2	1.86
W	1	2	< 1	1	1	2	2	2	1	1	3	2	1	5	2	2	< 1	0.3	-	-	2	1.59
Pb	53	84	144	27	65	127	57	45	67	71	17	33	53	66	22	26	-	-	-	-	18	19.3
Bi	< 0.4	< 0.4	< 0.4	< 0.4	< 0.4	< 0.4	< 0.4	< 0.4	< 0.4	0.4	< 0.4	< 0.4	< 0.4	< 0.4	< 0.4	< 0.4	< 0.4	0.03	-	-	0.6	0.56
Th	14.5	16.8	4.3	13.9	16.2	16.3	14.9	18.4	18.1	17.2	10.1	9.5	11.4	124	8.1	7.5	2.4	2.4	-	-	25.4	26.7
U	2.5	3.7	0.3	2.8	3.1	3.6	3.6	3.9	4.5	3.6	2.3	1.9	2.5	27.4	1.8	1.6	0.5	0.53	-	-	8.6	8.88

Notes: Major oxides are in weight per cent and trace elements in parts per million (ppm). Rock names (gph, granophyre; b.a., basaltic andesite; rhy, rhyolite; dac, dacite) are from the SINCLAS program of Verma *et al.* (2002) which uses LOI-free recalculated data and the TAS diagram of Le Bas *et al.* (1986). Samples BR4, AL4 and AL11 are dykes. LOI is loss in weight on ignition. 'Cert.' are the recommended values and 'Meas.' the measured values on USGS and CANMET reference materials.

Table 7. Sr and Nd isotopic data for rocks of the Barda and Alech complexes, Saurashtra

Sample	BR1	BR3	BR4	BR5	BR7	BR11	BR12	AL4	AL5	AL7	AL10	AL11
Location	Barda	Barda	Barda	Barda	Barda	Barda	Barda	Alech	Alech	Alech	Alech	Alech
Rock type	gph	gph	b.a.	gph	gph	gph	gph	rhy	rhy	dac	rhy	dac
Rb ppm	122	123	36	117	127	126	104	145	23	78	20	87
Sr ppm	84	65	135	62	65	52	69	59	18	77	191	157
Rb/Sr	1.452	1.892	0.267	1.887	1.954	2.423	1.507	2.458	1.278	1.013	0.105	0.554
$^{87}\text{Rb}/^{86}\text{Sr}$	4.203	5.476	0.772	5.461	5.654	7.011	4.361	7.111	3.697	2.931	0.303	1.603
$(^{87}\text{Sr}/^{86}\text{Sr})_p$	0.709946	0.711044	0.708104	0.711102	na	na	0.710204	0.712463	0.710794	0.709163	0.70674	0.707842
\pm	0.00002	0.00002	0.00002	0.00002	–	–	0.00002	0.00002	0.00002	0.00002	0.00002	0.00002
$(^{87}\text{Sr}/^{86}\text{Sr})_t$	0.706066	0.705988	0.707391	0.70606	na	na	0.706177	0.705897	0.70738	0.706457	0.70646	0.706361
Nd ppm	13.9	12.5	4.1	10.3	11.5	12.1	11.4	12.5	9.6	8.2	7.6	6.3
Sm ppm	64.2	54.2	15.3	44.1	50.1	53.5	51.3	61.7	42.9	37	35.7	30.1
Sm/Nd	0.2165	0.2306	0.268	0.2336	0.2295	0.2262	0.2222	0.2026	0.2238	0.2216	0.2129	0.2093
$^{147}\text{Sm}/^{144}\text{Nd}$	0.1309	0.1394	0.162	0.1412	0.1388	0.1367	0.1344	0.1225	0.1353	0.134	0.1287	0.1265
$(^{143}\text{Nd}/^{144}\text{Nd})_p$	0.512611	0.512673	0.511065	0.512661	0.51264	0.512667	0.512626	0.512707	0.512542	0.512562	0.512571	0.512571
\pm	0.00006	0.00006	0.00006	0.00006	0.00006	0.00006	0.00006	0.00006	0.00006	0.00006	0.00006	0.00006
$(^{143}\text{Nd}/^{144}\text{Nd})_t$	0.512556	0.512614	0.510996	0.512601	0.512581	0.512609	0.512569	0.512655	0.512485	0.512505	0.512516	0.512517
ϵNd_p	–0.5	0.7	–30.7	0.4	0	0.6	–0.2	1.3	–1.9	–1.5	–1.3	–1.3
ϵNd_t	0	1.2	–30.4	0.9	0.5	1.1	0.3	2	–1.4	–1	–0.7	–0.7

Notes: Samples BR4 (basaltic andesite), AL4 (rhyolite) and AL11 (dacite) are dykes, gph are granophyres.

The Sr and Nd isotopic data are age-corrected to 65 Ma using inductively coupled plasma mass spectrometer (ICP-MS) values of Rb, Sr, Sm and Nd. Epsilon Nd (ϵNd) values have been calculated for the rocks using a chondritic average value of $^{143}\text{Nd}/^{144}\text{Nd} = 0.512638$ and $^{147}\text{Sm}/^{144}\text{Nd} = 0.1967$ (present-day). Using the ages obtained in this study (such as 69 Ma instead of 65 Ma for the Barda granophyres) gives $(^{87}\text{Sr}/^{86}\text{Sr})_t$ ratios that are lower by 0.00004–0.00031 in the different samples, and makes no significant difference in the $(^{143}\text{Nd}/^{144}\text{Nd})_t$ ratios and ϵNd_t values.

Since most samples are not dated, 65 Ma is the preferred age for correcting present-day ratios and for direct comparison with previous studies.

'na' indicates not analysed/available.

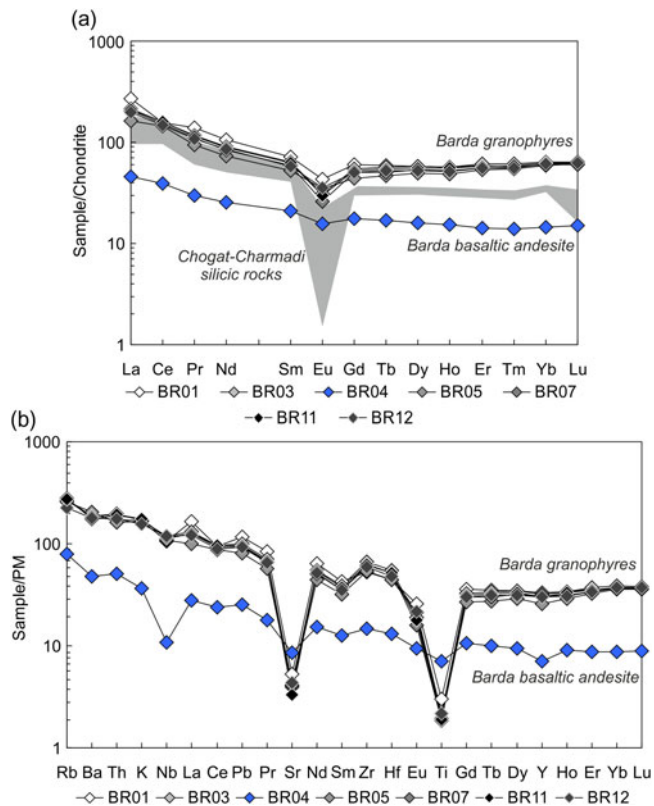


Fig. 7. (Colour online) (a) Chondrite-normalized REE patterns of the Barda rocks. Chondrite normalizing values are from Boynton (1984). Also shown for comparison are patterns of some silicic rocks of the Chogat-Chamardi complex (Sheth *et al.* 2011). (b) Primitive mantle-normalized multi-element patterns of the Barda rocks. Normalizing values are from Lyubetskaya & Korenaga (2007).

rhyolite (possibly also an ignimbrite) forming Chek Hill (226 m, Fig. 2), and AL11 is a dark grey, very fine-grained dyke cutting AL11. Both samples are visibly altered and have high LOI values (4.94 and 4.83 wt %, respectively). They have very similar Th, Nb, Zr, Hf, Ti and REE contents, as shown by their almost overlapping primitive mantle-normalized patterns in Figure 8c, but they differ considerably in Rb, Ba, K and Na, the fluid-mobile elements. The isotopic and trace element data indicate that rhyolite AL10 and the dacite dyke AL11 cutting it were both derived from the same magma reservoir.

6. Discussion

6.a. Emplacement ages

Field relationships (Dave, 1971; De & Bhattacharyya, 1971) and the ^{40}Ar - ^{39}Ar age data obtained in this study imply that the Barda granophyre plutons were emplaced at 69.5–68.5 Ma into Deccan basalt flows. The granophyre plutons and the local basalts thus significantly pre-date the intense 66–65 Ma Deccan flood basalt phase forming the bulk of the Deccan flood basalts, in the Western Ghats as well as the northern regions including Mount Pavagadh (Baksi, 2014; Renne *et al.* 2015; Schoene *et al.* 2015; Parisio *et al.* 2016). Generally, in widely separated areas of the Deccan province, field relationships (and ^{40}Ar - ^{39}Ar data) show silicic lavas and intrusions to have been emplaced after thick flood basalt sequences. The best examples are Mount Pavagadh (Chatterjee, 1961; Sheth & Melluso, 2008; Parisio *et al.* 2016), Osham Hill (Wakhaloo, 1967; Sheth *et al.* 2012) and Mumbai (Sheth & Pande, 2014). In other flood basalt

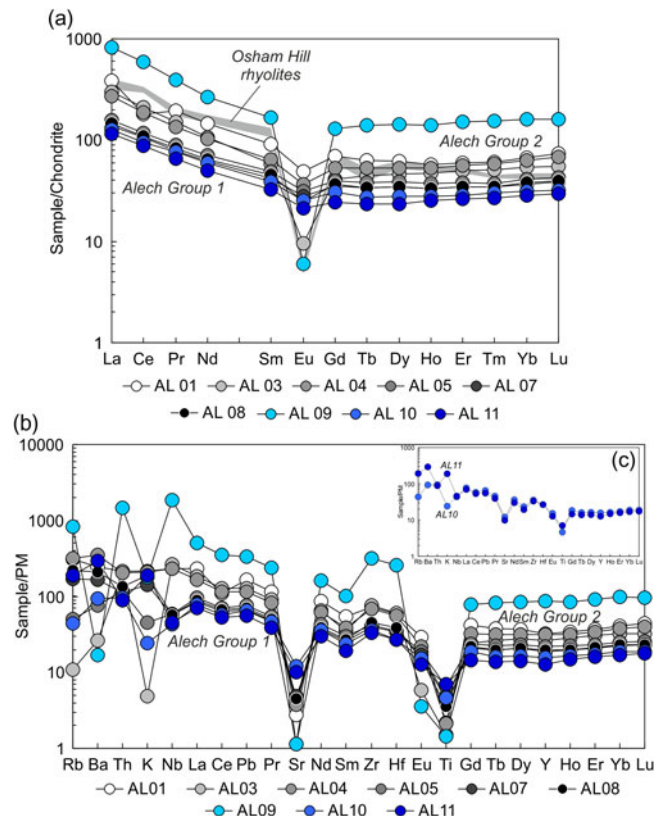


Fig. 8. (Colour online) (a) Chondrite-normalized REE patterns of the Alech rocks. Chondrite normalizing values are from Boynton (1984). Also shown for comparison are patterns of Osham Hill rhyolitic rocks (Sheth *et al.* 2012). (b) Primitive mantle-normalized multi-element patterns of the Alech rocks. Normalizing values are from Lyubetskaya & Korenaga (2007). (c) Comparison of the primitive mantle-normalized multi-element patterns of Chek Hill rhyolite AL10 and dacite dyke AL11, Alech complex.

provinces of the world (such as the Karoo) also, rhyolitic lavas and ignimbrites have generally erupted towards the close or at the end of the flood basalt volcanism (e.g. Melluso *et al.* 2008). The early silicic magmatism in the NW Deccan Traps, represented by the Barda granophyre plutonism, is therefore a novel result of this study.

We have not dated any of the Alech rocks because of their generally weathered nature, and therefore we do not know the age of emplacement of the complex relative to the main tholeiitic phase in the Deccan province at 66–65 Ma. However, the Alech complex, like the Barda complex, postdates the local Deccan basalt flows.

6.b. Petrogenesis

Silicic igneous rocks are common in intraplate extensional settings such as the Basin and Range province (e.g. Colgan *et al.* 2006), post-collisional extensional settings (e.g. Nedelec *et al.* 1995) and at rifted continental margins associated with CFB volcanism (e.g. Melluso *et al.* 2001, 2008; Cucciniello *et al.* 2010, 2011). These rocks provide important information on tectonic deformation and the generation, storage and transport of silicic magma in the continental lithosphere. Silicic rocks in general, and those in CFB provinces in particular, are known to be produced by several mechanisms, such as advanced fractional crystallization of mafic magmas (e.g. Turner *et al.* 1992; Soesoo, 2000; McCurry *et al.* 2008; Melluso *et al.* 2008), crustal assimilation with fractional crystallization (AFC) (e.g. Sheth & Melluso, 2008; Cucciniello *et al.* 2010), hybridization

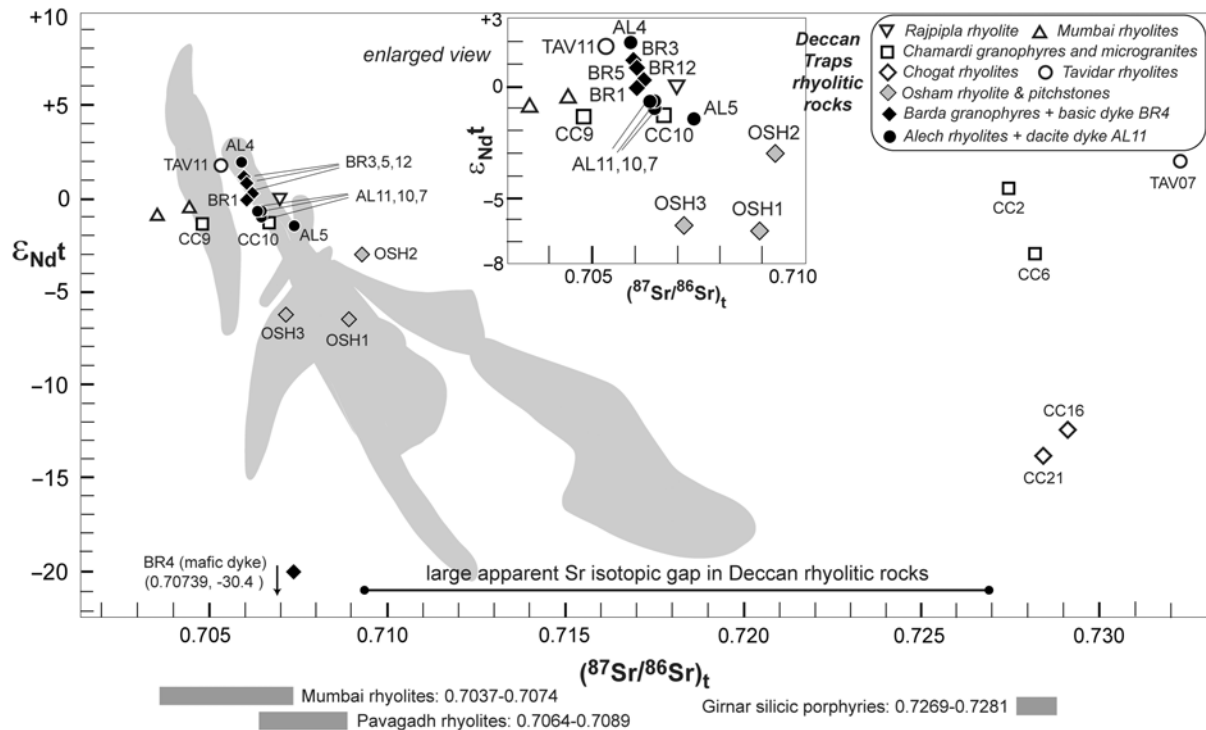


Fig. 9. Sr–Nd isotopic plot showing data for Deccan Traps silicic rocks, including the Barda–Alech silicic rocks (this study). Data sources are: Rajpipla rhyolite (Mahoney *et al.* 1985), Mumbai rhyolites (Lightfoot *et al.* 1987), Chamardi granophyres and microgranites and Choghat rhyolites (Sheth *et al.* 2011), Osham rhyolite and pitchstones (Sheth *et al.* 2012) and Tavidar rhyolites (Sen *et al.* 2012). Nd isotopic data are not available for the Pavagadh rhyolites (Sheth & Melluso, 2008), Mount Girnar silicic porphyry (Paul *et al.* 1977), and several other Mumbai rhyolites (Lightfoot *et al.* 1987), whose Sr isotopic ranges are shown by grey bands under the main figure. Also shown in the background are Sr–Nd isotopic compositions of the Western Ghats stratigraphic formations (light grey fields, Vanderkluyzen *et al.* 2011). All Sr–Nd isotopic data are initial ratios recalculated at 65 Ma and plotted for direct comparison. Note the large gap in Sr isotopic composition between the various silicic rocks. An enlarged view of the little-contaminated silicic rocks of the Deccan Traps, including the Barda–Alech samples of this study, is also provided as an inset figure.

between mantle-derived and crustally derived magmas (e.g. Wickham *et al.* 1996), partial melting of hydrothermally altered basic lavas or intrusions (e.g. Zellmer *et al.* 2008; Colón *et al.* 2015), and anatexis of old basement crust (e.g. Riley *et al.* 2001; Shellnutt *et al.* 2011, 2012; Zhu *et al.* 2017).

The data presented in this study show that the Barda granophyres are mainly metaluminous and have high Fe number [0.95–0.98; $\text{Fe}\# = \text{FeO}_t / (\text{FeO}_t + \text{MgO})$], Ga/Al (3.1–3.3) ratios, Zr, Nb and REE contents (Table 1). These geochemical characteristics (Ga/Al = 3.75; Zr = 528 ppm; Nb = 37 ppm) resemble those of A-type (ferroan) granitoids typical of within-plate settings (e.g. Whalen *et al.* 1987). Similarly, the Alech rhyolites and dacites have geochemical features typical of silicic rocks of within-plate settings (e.g. $\text{Fe}\# = 0.81\text{--}0.99$; Ga/Al = 2.6–5.5).

Direct derivation of the Barda–Alech silicic rocks by partial melting of old crustal rocks (e.g. western Indian Precambrian granites) is precluded by the Sr–Nd isotopic data, because these ancient granites have much higher $^{87}\text{Sr}/^{86}\text{Sr}$ ratios (e.g. 0.7690, Gopalan *et al.* 1979) than the Barda–Alech silicic rocks. Only the Barda basaltic andesite dyke BR4 has a very unradiogenic Nd isotopic composition ($\epsilon_{\text{Nd}} = -30.4$), similar to some ancient Indian granites (e.g. Jayananda *et al.* 2006). This simply reflects the incorporation of old basement crust in the dyke magma, possibly the same crust whose quartzitic xenoliths are still found in this dyke.

Basic amphibolites, in the presence of a free fluid phase, produce relatively silicic (tonalitic or trondhjemitic) partial melts over a wide melting range (5–30 kbar, 750–1100 °C; e.g. Van der Laan & Wyllie, 1991; Winther & Newton, 1991). However, the oldest exposed rocks in Saurashtra are Mesozoic sandstones, and no

drillholes into Precambrian basement exist, so it is unknown whether amphibolites exist there. Besides, Archaean basic amphibolites analysed from Rajasthan, NW India, have average $^{87}\text{Sr}/^{86}\text{Sr}$ of 0.7151 and ϵ_{Nd} of –12 (Gopalan *et al.* 1990), very unlike those of the Barda–Alech silicic rocks.

The absence of primary minerals, such as muscovite, cordierite, garnet, aluminosilicates (andalusite or sillimanite) and tourmaline, in the Barda–Alech rocks (and the presence of aegirine–augite in the Barda granophyres) also excludes an origin for these rocks as anatectic melts of metasedimentary protoliths. In addition, the Barda–Alech rocks have Zr and Y contents much higher than those normally observed in anatectic, S-type leucogranites from pelitic sources worldwide (e.g. Whalen *et al.* 1987; Bea *et al.* 1994).

Silicic magmas derived from partial melting of garnet granulites (e.g. Verma, 1999) or eclogites (e.g. Rapp *et al.* 2003) are characterized by low Y and HREE contents as a consequence of residual garnet (Schnetger, 1994). The high Y (>43 ppm) and HREE (e.g. $\text{Yb}_n > 17$) contents observed in the Barda–Alech silicic rocks thus rule out garnet granulite or eclogite sources.

Partial melting of previously emplaced basaltic rocks or gabbroic intrusions, likely hydrothermally altered, is also a plausible hypothesis for the genesis of silicic magmas. This mechanism can explain the absence of compositions intermediate between basalt and dacite–rhyolite, and the mantle-like Sr–Nd isotopic ratios of the Barda–Alech silicic rocks. However, experimental work shows that water-saturated melting of basaltic rocks, amphibolites and greenstones at 1, 3, 6.9 and 10 kbar pressure (Helz, 1976; Spulber & Rutherford, 1983; Beard & Lofgren, 1991; Wolf & Wyllie, 1994) should produce liquids ($\text{SiO}_2 = 65\text{--}75$ wt %) with

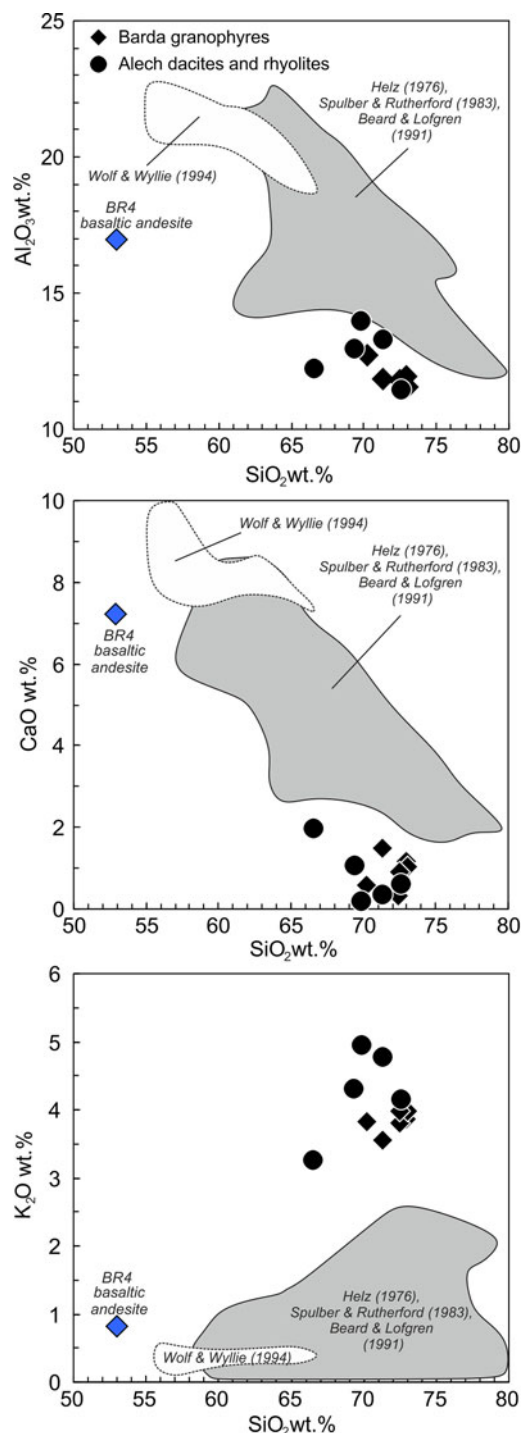


Fig. 10. (Colour online) Comparison of Barda–Alech silicic rock compositions with those of experimental liquids produced by partial melting of hydrated basaltic rocks, greenstones, and amphibolites. Fields enclose the experimental data of Wolf & Wyllie (1994), Beard & Lofgren (1991), Spulber & Rutherford (1983) and Helz (1976).

higher Al_2O_3 (>14 wt %) and CaO (>2 wt %) contents and lower K_2O (<2.5 wt %) contents than the Barda–Alech silicic rocks (Fig. 10). We were unable to reproduce the geochemical characteristics of the Barda–Alech silicic rocks by either fractional or batch melting mechanisms from a dry basaltic source, such as basaltic andesite BR4 composition, with no subsequent fractionation (Fig. 11). Partial melting models using other Deccan basalt compositions from

Saurashtra (Melluso *et al.* 1995) also fail to reproduce the geochemical characteristics of the Barda–Alech silicic rocks (Fig. 11).

The small range of Sr–Nd isotopic variation within the Barda granophyres ($(^{87}\text{Sr}/^{86}\text{Sr})_t = 0.705988\text{--}0.706066$, $\epsilon_{\text{Nd}t} = 0.0$ to +1.1) does not permit significant open-system processes and crustal incorporation within the Barda granophyres. The slight positive correlation between $(^{143}\text{Nd}/^{144}\text{Nd})_t$ and Nd concentrations, and the absence of Pb peaks and Nb troughs in mantle-normalized incompatible element patterns (Figs. 7b and 8b), also indicates that assimilation of crustal material was negligible in the genesis of the Barda granophyres and Alech samples AL1, 3, 4, 9 (group 2). Crustal contamination may have had some role in the genesis of the Alech samples AL5, 7, 8, 10, 11 (group 1) which have higher $(^{87}\text{Sr}/^{86}\text{Sr})_t$ of 0.706361–0.707379 and comparatively lower $\epsilon_{\text{Nd}t}$ values (–0.7 to –1.4), with Nb troughs in mantle-normalized incompatible element patterns.

We therefore suggest that a model of advanced, nearly-closed system fractional crystallization of early basaltic melts, stored in crustal magma chambers, can explain the production of the Barda–Alech silicic rocks. Trace element abundance patterns provide convincing evidence for derivation of the Barda granophyres and Alech rhyolites by fractional crystallization of basaltic magma. Negative anomalies of Ba, Sr and Eu in the mantle-normalized multi-element patterns of the silicic rocks are suggestive of fractionation of plagioclase feldspar, whereas negative Ti anomalies suggest fractionation of Ti-bearing oxides (Figs. 7b and 8b). Using the software Rhyolite-MELTS (Gualda *et al.* 2012) we calculated the liquid lines of descent of the magmas and the composition of the residual liquid (Fig. 12). Model results indicate that at QFM oxygen buffer conditions and 1–2 kbar pressure with $\text{H}_2\text{O} = 0.5\text{--}1.0$ wt %, the transition from basaltic andesite composition BR4 to a rhyolitic composition ($\text{SiO}_2 = 70.2\text{--}73.0$ wt %) involves 70 % fractional crystallization, with the crystal extract composed of plagioclase (58 %), clinopyroxene (25 %) and spinel (17 %). Fractional crystallization modelling using Rayleigh fractionation equations (Fig. 11) indicates that the Barda–Alech silicic rocks could be the result of nearly-closed system fractional crystallization (~70–75 %) of a low-Ti basaltic magma, in broad agreement with the Rhyolite-MELTS modelling results.

Note that liquid immiscibility did not have a role in the genesis of the Barda–Alech silicic rocks, as we infer from the absence of typical features of liquid immiscibility (such as Fe-rich globules, De, 1974) in the groundmass of basaltic andesite BR4.

The depth at which Barda–Alech silicic magmas were stored prior to their shallower-level intrusion or extrusion is difficult to assess, as the mineral assemblage is not suitable for geobarometry. However, the presence of a small amount of primary amphibole in some of the Barda silicic rocks (Dave, 1971; De & Bhattacharyya, 1971) indicates that the crystallizing magmas were hydrous. A semiquantitative estimate of the pressure of equilibration can be obtained using the synthetic system quartz–albite–orthoclase– H_2O (Fig. 13). The Barda granophyres plot close to the water-saturated minimum compositions at 2 kbar and 3 kbar. Pressures for the Alech magmas range from 1 atm to 5 kbar, with most values at the shallower end.

Residual rhyolitic melt forming by closed-system fractional crystallization of basalt represents a very small percentage of original liquid (e.g. Bowen, 1928; McCurry *et al.* 2008; Jagoutz & Klein, 2018). Whitaker *et al.* (2008) find that potassic rhyolitic melts can form by very advanced (96–97 %) closed-system fractional crystallization of olivine tholeiite melts with 10.6 wt % MgO. Many occurrences of small volumes of interstitial granophyric or rhyolitic

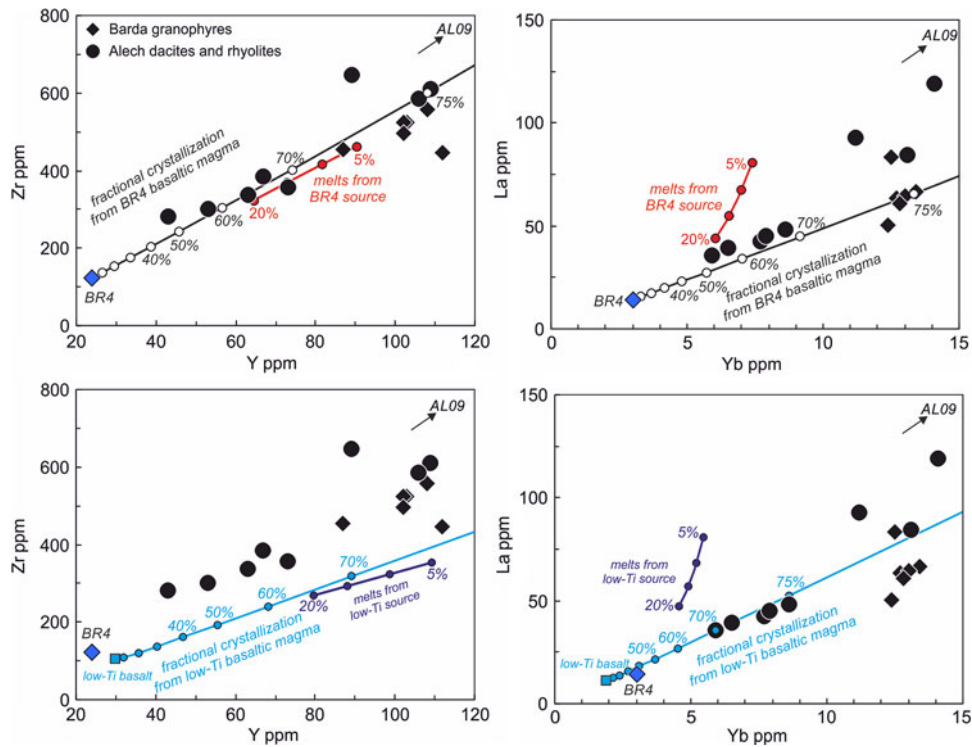


Fig. 11. (Colour online) Variation of Zr vs Y, and La vs Yb, for Barda–Alech silicic rocks compared with model results for batch partial melting of Deccan mafic rocks and closed-system fractional crystallization (FC) of Deccan mafic magmas. The values on the batch melting model are 5% melting increments for 5–20% melting. Fractional melting model results are similar to those of the batch melting model. Bulk distribution coefficients (D) have been estimated using the proportions of minerals in the fractional crystallization extracts (obtained from Rhyolite-MELTS calculations) in combination with mineral–liquid distribution coefficients from the literature (GERM website; <http://www.earthref.org>). The numbers close to the FC curves indicate the residual liquid fraction (f). Data sources are Melluso *et al.* (1995, low-Ti basalt) and this study (basaltic andesite BR4). The model source for batch melting has 40% plagioclase, 40% clinopyroxene, 10% olivine and 10% magnetite in the mode; melting of these minerals is assumed to occur in proportions of 75:15:5:5, respectively (Mahoney *et al.* 2008). The partition coefficients are from Mahoney *et al.* (2008).

melts are known from Deccan tholeiitic dykes and sills (e.g. Subba Rao, 1971; Sen, 1980). What is surprising therefore is the sheer volume of granophyre and rhyolite magma that is concentrated in the Barda and Alech complexes, derived from nearly-closed system fractional crystallization of basaltic magma. This requires a very large basaltic magma chamber in the crust beneath Saurashtra. Interestingly, the Barda and Alech complexes sit atop a pronounced, wide and roughly circular-shaped gravity high and magnetic anomaly (Chandrasekhar *et al.* 2002), which may indicate just such a mafic magma chamber in the upper crust (or several smaller, coalesced magma chambers). This anomaly is one of several circular-shaped gravity highs (of 40–60 mGal) and magnetic anomalies (of 800–1000 nT) mapped by Chandrasekhar *et al.* (2002) over the Saurashtra region. They modelled the Barda–Alech gravity–magnetic anomaly with mafic igneous material of density 2.88 g cm^{-3} in the upper crust, noting that such material in the denser lower crust would not generate an anomaly. Besides, the circular shape of the anomaly rules out Precambrian amphibolites or similar mafic rocks as its cause. Such rocks, if they exist in the Saurashtra crust, would have elongated (and commonly strongly folded) geometries, at all spatial scales, as well seen in surface outcrops in Rajasthan (e.g. Gupta *et al.* 1980).

Thus, we suggest that the Barda–Alech silicic rocks are the residual melts from advanced (70–75%) fractional crystallization in a large mafic magma chamber located in the upper crust under these complexes. The monzodiorite reported from Sajanwala Nes (De & Bhattacharyya, 1971) may represent an intermediate-stage product of the same process. Also, such a large chamber may have produced substantial crustal heating and melting. Our present sampling is necessarily limited, and it is probable that future intensive sampling of the Barda and Alech complexes, including in the high peaks of the former, may reveal many individual plutons or lavas with a substantial crustal input.

6.c. Genesis of silicic rocks of the Deccan Traps

Shellnutt *et al.* (2011) and Zhu *et al.* (2017), among others, have noted the coexistence of mantle-derived and crustally derived silicic magmas in parts of the Late Permian (260 Ma) Emeishan CFB province of China. Similarly, geochemical–isotopic data available for hitherto analysed silicic rocks of the Deccan Traps (Fig. 9) indicate a combination of these processes, sometimes even for a single rock suite (e.g. Subba Rao, 1971; Chatterjee & Bhattacharji, 2001; Sheth & Melluso, 2008; Sheth *et al.* 2011, 2012), as follows:

- Advanced fractional crystallization of basaltic magmas: The best example of this mechanism in the Deccan, involving little crustal interaction, is the Barda–Alech silicic rocks of the present study. Some Chogat–Chamardi silicic rocks also appear to have formed in this way (Sheth *et al.* 2011). Potassic rhyolites of Rajpipla (Krishnamurthy & Cox, 1980), one of which has been analysed for Sr–Nd isotopic composition (Mahoney *et al.* 1985), are also suitable candidates, as is a rhyolite from Tavidar in Rajasthan (Sen *et al.* 2012).
- Assimilation and fractional crystallization (AFC): In this process, progressively more fractionated melts are more crustally contaminated, as commonly observed in mafic–felsic suites. At Skye in the British Palaeogene igneous province, the granophyres have $(^{87}\text{Sr}/^{86}\text{Sr})_t$ values of 0.708–0.716, higher than for associated gabbros (0.703–0.709) (Moorbath & Bell, 1965). Similarly, granophyres in the Skaergaard Intrusion in East Greenland have higher Sr isotopic ratios than the bulk of the gabbros forming the intrusion (Leeman & Dasch, 1978). Silicic rocks in the Chogat–Chamardi complex are also much more contaminated than the associated gabbros and have been explained by AFC processes involving mafic magmas and old basement crust (Sheth *et al.* 2011). The Mount Pavagadh dacites and rhyolites have relatively high Zr (458–536 ppm),

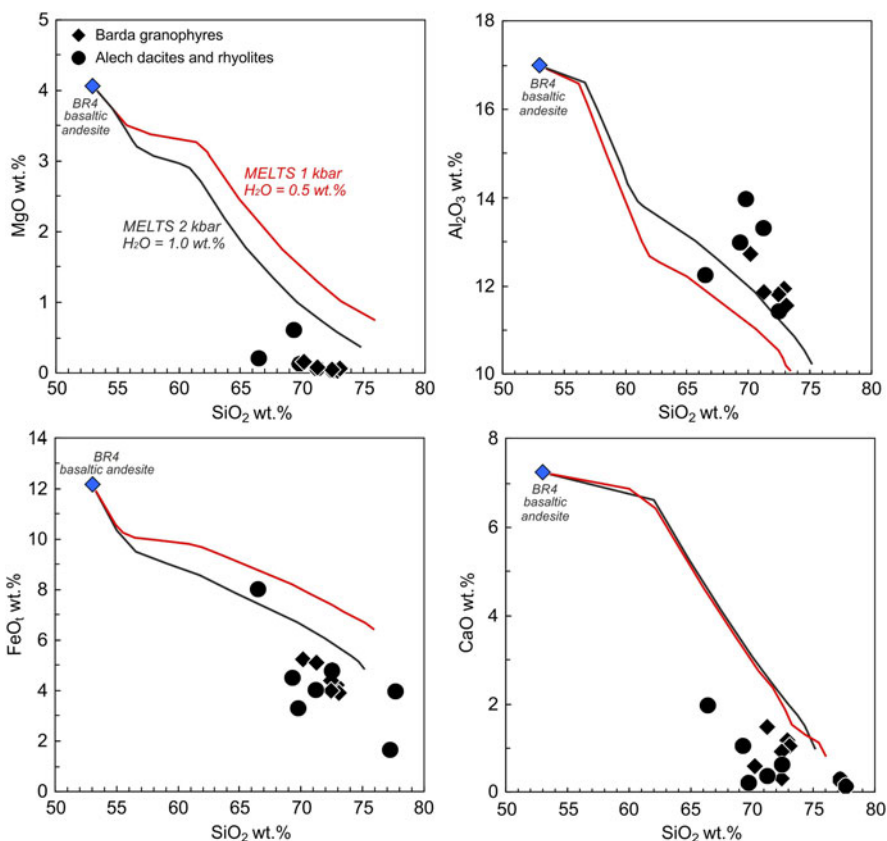


Fig. 12. (Colour online) Major (wt %) element composition of Barda and Alech rocks plotted vs SiO₂ (wt %). The black and red lines represent the fractional crystallization trends predicted by Rhyolite-MELTS software (Gualda *et al.* 2012). We performed isenthalpic runs using several sets of experimental conditions [P = 1–2 kbar, H₂O = 0.5–1 wt %, and fO₂ = QFM (quartz–fayalite–magnetite) buffer].

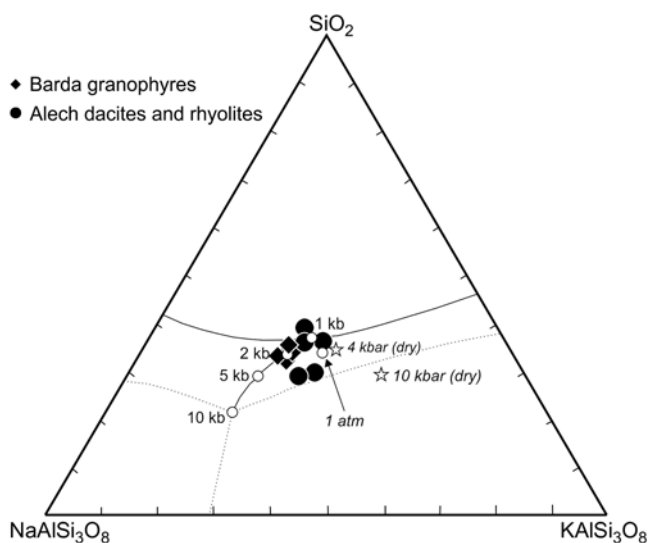


Fig. 13. Qtz–Ab–Or system with the compositions of the Barda–Alech silicic rocks plotted. The Qtz–Ab–Or proportions have been calculated from the rocks’ CIPW norms. The white circles correspond to water-saturated minima and eutectic compositions at 1 atm and 0.5–10 kbar (Schairer & Bowen, 1935; Tuttle & Bowen, 1958; Luth *et al.* 1964; Steiner *et al.* 1975). White triangles correspond to minima for the anhydrous system at 4 and 10 kbar (Huang & Wyllie, 1975; Steiner *et al.* 1975).

Nb (45–60 ppm) and Y (63–112 ppm) contents and are LREE-enriched ($La_n/Yb_n = 7.2–11.5$), and their $(^{87}Sr/^{86}Sr)_t$ varies from 0.70369 to 0.70826 (Sheth & Melluso, 2008). These authors modelled the silicic rocks by AFC involving a starting picritic magma and old felsic crust.

- (iii) Partial melting of hydrothermally altered basic lavas or intrusions: Lightfoot *et al.* (1987) proposed that Mumbai rhyolites, with high incompatible trace element contents (e.g. Zr = 1509–1801 ppm; Nb = 260–319 ppm; Y = 143–177 ppm), low $(^{87}Sr/^{86}Sr)_t$ ratios (0.7037–0.7074) and slightly negative $\epsilon_{Nd,t}$ values (–0.5 to –1.3) were derived by partial melting of basaltic intrusions in the crust due to heating by other intrusions (or by fractional crystallization of basaltic melts). The Osham Hill silicic lavas (Sheth *et al.* 2012) have low TiO₂ (0.12–0.10 wt %) and relatively high Zr (410–437 ppm) and Y (136–148 ppm) contents. They are LREE-enriched, with La_n/Yb_n ranging from 7.9 to 8.6. The Osham rhyolites have $\epsilon_{Nd,t} = -3.1$ to –6.5, and $(^{87}Sr/^{86}Sr)_t$ values from 0.70709 to 0.70927. Notably, these silicic lavas have the same Al₂O₃ contents as the underlying mafic flows, and therefore Sheth *et al.* (2012) considered an origin by fractional crystallization of mafic melts (i.e. involving substantial plagioclase) untenable. They suggested an origin of the Osham silicic lavas by partial melting of hydrothermally altered and K-metasomatized basaltic lavas or crustal intrusions, as proposed for some Icelandic rhyolites (Zellmer *et al.* 2008).
- (iv) Anatexis of old basement crust: A role for anatexis of ancient basement crust in the genesis of Deccan silicic magmas, as advocated by Subba Rao (1971), appears valid for some of the Rajula rhyolites (Chatterjee & Bhattacharji, 2001, 2004). It also seems valid for several of the Chogat–Chamardi granophyres and rhyolites (Sheth *et al.* 2011), which have TiO₂ in the range 0.26–1.1 wt % and moderate to high Zr (373–1209 ppm) and Y (69–117 ppm) contents, and are LREE-enriched, with La_n/Yb_n of 3.0–5.0. Their $(^{87}Sr/^{86}Sr)_t$ ratios are higher than 0.7275, and $\epsilon_{Nd,t}$ values range from +0.6 and –3.0 (Chamardi granophyres) to as low as –12.4 and –13.9

(Chogat rhyolites). The Tavidar rhyolite Tav07 may owe its very high $(^{87}\text{Sr}/^{86}\text{Sr})_t$ to weathering, however (Sen *et al.* 2012).

Considered as a whole, Sr isotopic data for the Deccan silicic rocks hitherto available show a large gap, from about 0.7095 to 0.7275 (Fig. 9), separating those with little or no crustal input from those with very strong crustal input or of entirely crustal derivation. Nd isotopic compositions of the rocks show much greater continuity than Sr isotopic compositions.

7. Conclusions

The Barda and Alech complexes in the Saurashtra region of the Deccan CFB province, India, are the largest silicic complexes in this province. The Barda complex is mainly composed of coalesced granophyre plutons. The Alech complex is made up dominantly of rhyolite and dacite which are probably ring-fracture lavas and lava-like ignimbrites. Despite early studies (Adye, 1914; Dave, 1971; De & Bhattacharyya, 1971), neither complex has received much study by modern geoanalytical methods.

In this study we have provided basic geological information on both complexes, which we hope to substantially expand on in the future. We have also provided petrographic and mineral chemical data and whole-rock geochemical (major and trace element and Sr–Nd isotopic) data, and ^{40}Ar – ^{39}Ar ages of three Barda granophyres. These ages indicate that the Barda granophyre intrusions are 69.5–68.5 Ma in age, and they and the Deccan basalt flows they intrude are thus significantly older (by 3–4 My) than the major 66–65 Ma flood basalt eruptive phase in the Deccan province (Baksi, 2014; Renne *et al.* 2015; Schoene *et al.* 2015; Parisio *et al.* 2016). Whereas silicic magmatism (lava flows and intrusions) typically postdates thick sequences of flood basalts in the Deccan Traps, as well as in other CFB provinces of the world, the early silicic magmatism represented by the Barda granophyre plutonism is a novel result of considerable interest. It also indicates that the total duration of Deccan magmatism was no less than 8 Ma (see e.g. Sheth & Pande, 2014 and references therein).

Though xenoliths of probable basement crust (the only ones known so far from Saurashtra) are present in a basaltic andesite dyke cutting the Barda granophyres, geochemical–isotopic data show little involvement of ancient basement crust in the genesis of the Barda–Alech silicic rocks. These data show that partial melting of several types of old basement lithologies (Indian Precambrian granitoids, amphibolites, metasedimentary rocks, garnetiferous granulites or granites), or partial melting of Deccan-age basaltic lavas or gabbro intrusions (possibly hydrothermally altered) within the Saurashtra crust, cannot have produced the Barda–Alech silicic rocks.

On the other hand, the geochemical–isotopic data indicate derivation of the Barda–Alech silicic rocks by prolonged, nearly-closed system fractional crystallization from low-Ti basaltic magmas stored in magma chambers located in the upper or middle crust. From the size of the Barda and Alech complexes (each tens of kilometres in diameter), a very large mafic magma chamber is indicated, and is reflected in the pronounced, circular-shaped gravity high and magnetic anomaly mapped over these complexes (Chandrasekhar *et al.* 2002).

The 69–68 Ma Barda granophyre plutonism took place in a within-plate setting, and along what was to become a future (62.5 Ma) rifted continental margin (Bhattacharya & Yatheesh, 2015). The Barda granophyre plutonism may be viewed in the larger context of subaerial to shallow-marine 75–68 Ma volcanism

that occurred WNW of Saurashtra, forming the Saurashtra Volcanic Platform (Calvès *et al.* 2011; Bhattacharya & Yatheesh, 2015). The voluminous, basalt fractionation-derived silicic magmatism in the Barda and Alech complexes is important in understanding the temporal evolution of Deccan flood basalt volcanism, and the genesis of silicic magmas in CFB provinces and in anorogenic, intraplate settings in general.

Supplementary material. To view supplementary material for this article, please visit <https://doi.org/10.1017/S0016756818000924>.

Author ORCIDs.  [Ciro Cucciniello 0000-0003-1908-0963](https://orcid.org/0000-0003-1908-0963)

Acknowledgements. Field work was supported by the Industrial Research and Consultancy Centre (IRCC, IIT Bombay) grant 09YIA001 to Sheth. Many thanks to Sergio Bravi for the preparation of thin sections and to Roberto de' Gennaro for his assistance in microprobe work. Funds for EPMA and whole-rock analyses by Cucciniello were provided by Italian MIUR (PRIN 2015, 20158A9CBM to L. Melluso) and Fondi Ricerca di Ateneo (DR_3450_2016 to C. Cucciniello). Pande acknowledges Grant No. IR/S4/ESF-04/2003 from the Department of Science and Technology (Government of India) towards the development of the IIT Bombay–DST National Facility for ^{40}Ar – ^{39}Ar Geo-thermochronology. He also thanks the IRCC, IIT Bombay, for maintenance support to the Facility (grant no. 151RCCCF04). We thank Nilanjan Chatterjee for valuable critical comments on an earlier version of this work. Constructive reviews of the present paper by Greg Shellnutt and Sheila Seaman and the editorial handling of Chad Deering are much appreciated.

References

- Adye EH (1914) *Economic Geology of the Nawanagar State in the Province of Kathiawar, India*. Mumbai: Thacker and Company, 262 pp.
- Auden JB (1949) Dykes in western India – a discussion of their relationships with the Deccan traps. *Transactions of the National Academy of Sciences of India* 3, 123–57.
- Baksi AK (2014) The Deccan trap–Cretaceous–Palaeogene boundary connection: new $^{40}\text{Ar}/^{39}\text{Ar}$ ages and critical assessment of existing argon data pertinent to this hypothesis. In *Flood Basalts of Asia* (eds HC Sheth and L Vanderkluyzen), pp. 9–23. *Journal of Asian Earth Sciences* no. 84.
- Bea F, Pereira MD and Stroth A (1994) Mineral/leucosome trace element partitioning in a peraluminous migmatite (a laser ablation ICP-MS study). *Chemical Geology* 117, 291–312.
- Beard JS and Lofgren GE (1991) Dehydration melting and water-saturated melting of basaltic and andesitic greenstones and amphibolites at 1, 3 and 6.9 kb. *Journal of Petrology* 32, 365–401.
- Bhattacharya GC and Yatheesh Y (2015) Plate-tectonic evolution of the deep ocean basins adjoining the western continental margin of India – a proposed model for the early opening scenario. In *Petroleum Geoscience: Indian Contexts* (ed. S Mukherjee), pp. 1–61. Cham: Springer.
- Bowen NL (1928) *The Evolution of the Igneous Rocks*. Princeton, New Jersey: Princeton University Press, 334 pp.
- Boydton WB (1984) Cosmochemistry of rare earth elements: meteorite studies. In: *Rare Earth Element Geochemistry* (ed P Henderson), pp. 63–114. Amsterdam: Elsevier.
- Calvès G, Schwab AM, Huuse M, Clift PD, Gaina C, Jolley D, Tabrez AR and Inam A (2011) Seismic volcanostratigraphy of the western Indian rifted margin: the pre-Deccan igneous province. *Journal of Geophysical Research* 116, 28.
- Chandrasekhar DV, Mishra DC, Poornachandra Rao GVS and Mallikharjuna Rao J (2002) Gravity and magnetic signatures of volcanic plugs related to Deccan volcanism in Saurashtra, India and their physical and geochemical properties. *Earth and Planetary Science Letters* 201, 277–92.
- Chatterjee AC (1961) Petrology of the lavas of Pavagad Hill, Gujarat. *Journal of the Geological Society of India* 2, 61–77.
- Chatterjee N and Bhattacharji S (2001) Origin of the felsic and basaltic dykes and flows in the Rajula–Palitana–Sihor area of the Deccan Traps, Saurashtra, India: a geochemical and geochronological study. *International Geology Review* 43, 1094–1116.

- Chatterjee N and Bhattacharji S** (2004) A preliminary geochemical study of zircons and monazites from Deccan felsic dykes, Rajula, Gujarat, India: implications for crustal melting. In *Magmatism in India through Time* (eds HC Sheth and K Pande), pp. 533–42. Bangalore: Proceedings of the Indian Academy of Sciences (Earth and Planetary Sciences) no. 113.
- Chatterjee SK** (1932) Igneous rocks from west Gir forest, Kathiawar. *The Journal of Geology* **40**, 155–60.
- Cleverly RW, Betton PJ and Bristow JW** (1984) Geochemistry and petrogenesis of the Lebombo rhyolites. In *Petrogenesis of the Volcanic Rocks of the Karoo Province* (ed. AJ Erlank), pp. 171–94. Johannesburg: Geological Society of South Africa Special Publication no. 13.
- Coble MA and Mahood GA** (2012) Initial impingement of the Yellowstone plume located by widespread silicic volcanism contemporaneous with Columbia River flood basalts. *Geology* **40**, 655–8.
- Colgan JP, Dumitru TA, McWilliams M and Miller EL** (2006) Timing of Cenozoic volcanism and Basin and range extension in northwestern Nevada: new constraints from the northern Pine forest range. *Geological Society of America Bulletin* **118**, 126–39.
- Colón DP, Bindeman IP, Ellis BS, Schmitt AK and Fisher CM** (2015) Hydrothermal alteration and melting of the crust during the Columbia River Basalt-Snake River plain transition and the origin of low- $\delta^{18}\text{O}$ rhyolites of the central Snake River Plain. *Lithos* **224–225**, 310–23.
- Cucciniello C, Conrad J, Grifa C, Melluso L, Mercurio M, Morra V, Tucker RD and Vincent M** (2011) Petrology and geochemistry of Cretaceous mafic and silicic dykes and spatially associated lavas in central-eastern coastal Madagascar. In *Dyke Swarms: Keys for Geodynamic Interpretation* (ed. RK Srivastava), pp. 345–75. Berlin: Springer Verlag.
- Cucciniello C, Demonerova EI, Sheth H, Pande K and Vijayan A** (2015) $^{40}\text{Ar}/^{39}\text{Ar}$ geochronology and geochemistry of the Central Saurashtra mafic dyke swarm: insights into magmatic evolution, magma transport, and dyke-flow relationships in the northwestern Deccan Traps. *Bulletin of Volcanology* **77**, 45.
- Cucciniello C, Langone A, Melluso L, Morra V, Mahoney JJ, Meisel T and Tiepolo M** (2010) U–Pb ages, Pb–Os isotopes ratios, and platinum-group element (PGE) composition of the West-Central Madagascar flood basalt province. *Journal of Geology* **118**, 523–41.
- Dave SS** (1971) The geology of the igneous complex of the Barda Hills, Saurashtra, Gujarat state (India). *Bulletin of Volcanology* **35**, 619–32.
- De A** (1974) Silicate liquid immiscibility in the Deccan traps and its petrogenetic significance. *Geological Society of America Bulletin* **85**, 471–4.
- De A** (1981) Late Mesozoic–Lower Tertiary magma types of Kutch and Saurashtra. In *Deccan Volcanism* (eds KV Subbarao and RN Sukheswala), pp. 327–39. Bangalore: Geological Society of India Memoir no. 3.
- De A and Bhattacharyya D** (1971) Phase-petrology with special reference to pyroxenes of the acid igneous complex of Barda Hills, western Saurashtra (Gujarat). *Bulletin of Volcanology* **35**, 907–29.
- Ellis BS, Wolff JA, Borroughs S, Mark DF, Starkel WA and Bonnicksen B** (2013) Rhyolitic volcanism of the central Snake river plain: a review. *Bulletin of Volcanology* **75**, 745.
- Fedden F** (1884) *The Geology of the Kathiawar Peninsula in Gujarat*. Calcutta: Geological Survey of India Memoir 21, Pt 2.
- Garland FE, Hawkesworth CJ and Mantovani MSM** (1995) Description and petrogenesis of the Paraná rhyolites. *Journal of Petrology* **36**, 1193–227.
- Gopalan K, Macdougall JD, Roy AB and Murali AV** (1990) Sm–Nd evidence for 3.3 Ga old rocks in Rajasthan, northwestern India. *Precambrian Research* **48**, 287–97.
- Gopalan K, Trivedi JR, Merh SS, Patel PP and Patel SG** (1979) Rb–Sr age of Godhra and related granites, Gujarat, India. *Proceedings of the Indian Academy of Sciences (Earth and Planetary Sciences)* **4**, 7–17.
- Gualda GAR, Ghorso MS, Lemons RV and Carley TL** (2012) Rhyolite-MELTS: a modified calibration of MELTS optimized for silica rich, fluid-bearing magmatic systems. *Journal of Petrology* **53**, 875–90.
- Gupta SN, Arora YK, Mathur RK, Iqbaluddin PB, Sahai TN and Sharma SB** (1980) *Lithostratigraphic Map of the Aravalli Region*. Kolkata: Geological Survey of India.
- Helz RT** (1976) Phase relations of basalts in their melting ranges at $P_{\text{H}_2\text{O}} = 5$ kb. Part II: Melt compositions. *Journal of Petrology* **17**, 139–93.
- Huang WL and Wyllie PJ** (1975) Melting reactions in the system $\text{NaAlSi}_3\text{O}_8\text{--KAlSi}_3\text{O}_8\text{--SiO}_2$, to 35 kilobars, dry and with excess water. *Journal of Geology* **83**, 737–48.
- Jagoutz O and Klein B** (2018) On the importance of crystallization-differentiation for the generation of SiO_2 -rich melts and the compositional build-up of arc (and continental) crust. *American Journal of Science* **318**, 29–63.
- Jayananda M, Chardon D, Peucat JJ and Capdevila R** (2006) 2.61 Ga potassic granites and crustal reworking in the western Dharwar craton, south India: tectonic, geochronologic and geochemical constraints. *Precambrian Research* **150**, 1–26.
- Krishnamacharlu T** (1972) Petrology of microdolerites from the Dedan cluster, Gujarat. *Journal of Geological Society of India* **13**, 262–72.
- Krishnamurthy P and Cox KG** (1977) Picrite basalts and related lavas from the Deccan Traps of western India. *Contributions to Mineralogy and Petrology* **62**, 53–75.
- Krishnamurthy P and Cox KG** (1980) A potassium-rich alkalic suite from the Deccan Traps, Rajpipla, India. *Contributions to Mineralogy and Petrology* **73**, 179–89.
- Krishnan MS** (1926) *The Petrography of Rocks from the Girnar and Osham Hills, Kathiawar*. Records of the Geological Survey of India **58**, 380 pp.
- Le Bas MJ, Le Maître RW, Streckeisen A and Zanettin P** (1986) A chemical classification of volcanic rocks based on the total alkali-silica diagram. *Journal of Petrology* **27**, 745–50.
- Leeman WP and Dasch EJ** (1978) Strontium, lead and oxygen isotopic investigation of the Skaergaard intrusion, east Greenland. *Earth and Planetary Science Letters* **41**, 47–51.
- Lele VS** (1973) The Miliolite Limestone of Saurashtra, western India. *Sedimentary Geology* **10**, 301–10.
- Lepage LD** (2003) ILMAT: an Excel worksheet for ilmenite–magnetite geothermometry and geobarometry. *Computers and Geosciences* **29**, 673–8.
- Lightfoot PC, Hawkesworth CJ and Sethna SF** (1987) Petrogenesis of rhyolites and trachytes from the Deccan Trap: Sr, Nd, and Pb isotope and trace element evidence. *Contributions to Mineralogy and Petrology* **95**, 44–54.
- Ludwig KR** (2012) *Isoplot/Ex*, v. 3.75. Berkeley, California: Berkeley Geochronology Center Special Publication No. 5.
- Luth WC, Jahns RH and Tuttle OF** (1964) The granite system at pressures of 4 to 10 kilobars. *Journal of Geophysical Research* **69**, 759–73.
- Lyubetskaya T and Korenaga J** (2007) Chemical composition of Earth's primitive mantle and its variance: 1. Method and results. *Journal of Geophysical Research* **112**, B03211. doi: [10.1029/2005JB004223](https://doi.org/10.1029/2005JB004223).
- Mahoney JJ, Macdougall JD, Lugmair GW, Gopalan K and Krishnamurthy P** (1985) Origin of contemporaneous tholeiitic and K-rich alkalic lavas: a case study from the northern Deccan Plateau, India. *Earth and Planetary Science Letters* **72**, 39–53.
- Mahoney JJ, Saunders AD, Storey M and Randriamanantenasoa A** (2008) Geochemistry of the Volcan de l'Androy basalt-rhyolite complex, Madagascar Cretaceous igneous province. *Journal of Petrology* **49**, 1069–96.
- Maithani PB, Goyal N, Banerjee R, Gurjar R, Ramchandran S and Singh R** (1996) Rhyolites of Osham hills, Saurashtra, India: a geochemical study. *Gondwana Geological Magazine Special Volume* **2**, 213–24.
- Marathe AR, Rajaguru SN and Lele VS** (1977) On the problem of the origin and age of the Miliolite rocks of the Hiran valley, Saurashtra, India. *Sedimentary Geology* **19**, 197–215.
- Mathur KK, Dubey VS and Sharma NL** (1926) Magmatic differentiation in Mount Girnar. *The Journal of Geology* **34**, 289–307.
- McCurry M, Hayden KP, Morse LH and Mertzman S** (2008) Genesis of post-hotspot, A-type rhyolite of the Eastern Snake River Plain volcanic field by extreme fractional crystallization of olivine tholeiite. *Bulletin of Volcanology* **70**, 361–83.
- Melluso L, Becalulla L, Brotzu P, Gregnanin A, Gupta AK, Morbidelli L and Traversa G** (1995) Constraints on the mantle sources of the Deccan Traps from the petrology and geochemistry of the basalts of Gujarat State (western India). *Journal of Petrology* **36**, 1393–432.
- Melluso L, Cucciniello C, Petrone CM, Lustrino M, Morra V, Tiepolo M and Vasconcelos L** (2008) Petrology of Karoo volcanic rocks in the southern Lebombo monocline, Mozambique. *Journal of African Earth Sciences* **52**, 139–51.

- Melluso L, Morra V, Brotzu P and Mahoney JJ** (2001) The Cretaceous igneous province of Madagascar: geochemistry and petrogenesis of lavas and dikes from the central-western sector. *Journal of Petrology* **42**, 1249–78.
- Misra KS** (1981) The tectonic setting of Deccan volcanics in southern Saurashtra and northern Gujarat. In *Deccan Volcanism* (eds KV Subbarao and RN Sukheswala), pp. 81–6. Bangalore: Geological Society of India Memoir no. 3.
- Moorbath S and Bell JD** (1965) Strontium isotope abundance studies and rubidium-strontium age determinations on Tertiary igneous rocks from the Isle of Skye, north-west Scotland. *Journal of Petrology* **6**, 37–66.
- Nedelec A, Stephens WE and Fallick AE** (1995) The Panafrican stratoid granites of Madagascar: alkaline magmatism in a post-collisional extensional setting. *Journal of Petrology* **36**, 1367–91.
- Owen-Smith TM, Ashwal LD, Torsvik TH, Ganerød M, Nebel O, Webb SJ and Werner S** (2013) Seychelles alkaline suite records the culmination of Deccan Traps continental flood volcanism. *Lithos* **182–183**, 33–47.
- Parisio L, Jourdan F, Marzoli A, Melluso L, Sethna SF and Bellieni G** (2016) $^{40}\text{Ar}/^{39}\text{Ar}$ ages of alkaline and tholeiitic rocks from the northern Deccan Traps: implications for magmatic processes and the K-Pg boundary. *Journal of the Geological Society of London* **173**, 679–88.
- Paul DK, Potts PJ, Rex DC and Beckinsale RD** (1977) Geochemical and petrogenetic study of the Girnar igneous complex, Deccan volcanic province, India. *Geological Society of America Bulletin* **88**, 227–34.
- Pouchou JL and Pichoir F** (1988) A simplified version of the “PAP” model for matrix corrections in EPMA. In *Microbeam Analysis* (ed. DE Newbury), pp. 315–18. San Francisco: San Francisco Press.
- Putirka K** (2008) Thermometers and barometers for volcanic systems. In *Minerals, Inclusions and Volcanic Processes* (eds K Putirka and F Tepley), pp. 61–120. Washington, DC: Reviews in Mineralogy and Geochemistry 69, American Mineralogical Society.
- Rapp RP, Shimizu N and Norman MD** (2003) Growth of early continental crust by partial melting of eclogite. *Nature* **425**, 605–9.
- Renne PR, Sprain CJ, Richards MA, Self S, Vanderkluysen L and Pande K** (2015) State shift in Deccan volcanism at the Cretaceous-Paleogene boundary, possibly induced by impact. *Science* **350**(6256), 76–78. doi: [10.1126/science.aac7549](https://doi.org/10.1126/science.aac7549)
- Renne PR, Swisher CC, Deino AL, Karner DB, Owens TL and DePaolo DJ** (1998) Intercalibration of standards, absolute ages and uncertainties in $^{40}\text{Ar}/^{39}\text{Ar}$ dating. *Chemical Geology* **145**, 117–52.
- Riley TR, Leat PT, Pankhurst RJ and Harris C** (2001) Origins of large-volume rhyolitic volcanism in the Antarctic Peninsula and Patagonia by crustal melting. *Journal of Petrology* **42**, 1043–65.
- Schairer JF and Bowen NL** (1935) Preliminary report on equilibrium relations between feldspathoids, alkali feldspars, and silica. *Transactions of the American Geophysical Union* **16**, 325–8.
- Schnetger B** (1994) Partial melting during the evolution of the amphibolite- to granulite-facies gneisses of the Ivrea Zone, northern Italy. *Chemical Geology* **113**, 71–101.
- Schoene B, Samperton KM, Eddy MP, Keller G, Adatte T, Bowring S, Khadri SFR and Gertsch B** (2015) U-Pb geochronology of the Deccan Traps and relation to the end-Cretaceous mass extinction. *Science* **347**, 182–4.
- Sen G** (1980) Mineralogical variations in the Delakhari Sill, Deccan Trap intrusion, central India. *Contributions to Mineralogy and Petrology* **75**, 71–8.
- Sen A, Pande H, Hegner E, Sharma KK, Dayal AM, Sheth HC and Mistry H** (2012) Deccan volcanism in Rajasthan: ^{40}Ar - ^{39}Ar geochronology and geochemistry of the Tavidar volcanic suite. *Journal of Asian Earth Sciences* **59**, 127–40.
- Shellnutt JG, Bhat GM, Wang K-L, Brookfield ME, Dostal J and Jahn B-M** (2012) Origin of the silicic volcanic rocks of the Early Permian Panjal Traps, Kashmir, India. *Chemical Geology* **334**, 154–70.
- Shellnutt JG, Jahn B-M and Zhou M-F** (2011) Crustally-derived granites in the Panzhuhua region, SW China: implications for felsic magmatism in the Emeishan Large Igneous province. *Lithos* **123**, 145–57.
- Shellnutt JG, Yeh M-W, Suga K, Lee T-Y, Lee H-Y and Lin T-H** (2017) Temporal and structural evolution of the early Palaeogene rocks of the Seychelles micro-continent. *Scientific Reports* **7**, 179. doi: [10.1038/s41598-017-00248-y](https://doi.org/10.1038/s41598-017-00248-y).
- Sheth HC, Choudhary AK, Bhattacharyya S, Cucciniello C, Laishram R and Gurav T** (2011) The Chogat-Chamardi subvolcanic complex, Saurashtra, northwestern Deccan Traps: geology, petrochemistry, and petrogenetic evolution. *Journal of Asian Earth Sciences* **41**, 307–24.
- Sheth HC, Choudhary AK, Cucciniello C, Bhattacharyya S, Laishram R and Gurav T** (2012) Geology, petrochemistry, and genesis of the bimodal lavas of Osham Hill, Saurashtra, northwestern Deccan Traps. *Journal of Asian Earth Sciences* **43**, 176–92.
- Sheth HC and Melluso L** (2008) The Mount Pavagadh volcanic suite, Deccan Traps: geochemical stratigraphy and magmatic evolution. *Journal of Asian Earth Sciences* **32**, 5–21.
- Sheth HC and Pande K** (2014) Geological and $^{40}\text{Ar}/^{39}\text{Ar}$ age constraints on late-stage Deccan rhyolitic volcanism, inter-volcanic sedimentation, and the Panvel flexure from the Dongri area, Mumbai. In *Flood Basalts of Asia* (eds HC Sheth and L Vanderkluysen), pp. 167–75. Journal of Asian Earth Sciences no. 84.
- Soesoo A** (2000) Fractional crystallization of mantle-derived melts as a mechanism for some I-type granite petrogenesis: an example from Lachlan fold belt, Australia. *Journal of the Geological Society, London* **157**, 135–49.
- Spulber SD and Rutherford MJ** (1983) The origin of rhyolite and plagiogranite in oceanic crust: an experimental study. *Journal of Petrology* **24**, 1–25.
- Steiner JC, Jahns RH and Luth WC** (1975) Crystallization of alkali feldspar and quartz in the haplogranite system $\text{NaAlSi}_3\text{O}_8$ - KAlSi_3O_8 - SiO_2 - H_2O at 4 kb. *Geological Society of America Bulletin* **86**, 83–98.
- Subba Rao S** (1971) Petrogenesis of acid rocks of the Deccan Traps. *Bulletin of Volcanology* **35**, 983–97.
- Turner SP, Foden JD and Morrison RS** (1992) Derivation of some A-type magmas by fractionation of basaltic magma: an example from the Padthaway Ridge, South Australia. *Lithos* **28**, 151–79.
- Tuttle OF and Bowen NL** (1958) Origin of granite, in the light of experimental studies in the system $\text{NaAlSi}_3\text{O}_8$ - KAlSi_3O_8 - SiO_2 - H_2O . *Geological Society of America Memoir* **74**, 153.
- Van der Laan SR and Wyllie PJ** (1991) Constraints on Archaean trondhjemite genesis from hydrous crystallization experiments on Nuk gneiss at 10–17 kbar. *Journal of Geology* **100**, 57–68.
- Vanderkluysen L, Mahoney JJ, Hooper PR, Sheth HC and Ray R** (2011) The feeder system of the Deccan Traps (India): insights from dyke geochemistry. *Journal of Petrology* **52**, 315–43.
- Verma SP** (1999) Geochemistry of evolved magmas and their relationship to subduction-unrelated mafic volcanism at the volcanic front of the central Mexican Volcanic Belt. *Journal of Volcanology and Geothermal Research* **93**, 151–71.
- Verma SP, Torres-Alvarado IS and Sotelo-Rodriguez ZT** (2002) SINCLAS: Standard igneous norm and volcanic rock classification system. *Computers and Geosciences* **28**, 711–15.
- Wakhaloo SN** (1967) On the nature of volcanic eruption and of differentiation of the Girnar igneous complex, Junagarh, Kathiawar peninsula, India. In *Proceedings of Symposium on Upper Mantle Project, Hyderabad*, pp. 430–49. Hyderabad: National Geophysical Research Institute, India.
- West WD** (1958) The petrography and petrogenesis of forty-eight flows of Deccan Trap penetrated by borings in western India. *Transactions of the National Institute of Sciences (India)* **4**, 1–56.
- Whalen JB, Currie KL and Chappell BW** (1987) A-type granites: geochemical characteristics, discrimination and petrogenesis. *Contributions to Mineralogy and Petrology* **95**, 407–19.
- Whitaker ML, Nekvasil H, Lindsley DH and McCurry M** (2008) Can crystallization of olivine tholeiite give rise to potassic rhyolites? – an experimental investigation. *Bulletin of Volcanology* **70**, 417–34.
- Wickham SM, Alberts AD, Litvinovsky BA, Bindeman IN and Schauble EA** (1996) A stable isotope study of anorogenic magmatism in East Central Asia. *Journal of Petrology* **37**, 1063–95.
- Winther KC and Newton RC** (1991) Experimental melting of hydrous low-K tholeiite: evidence on the origin of Archaean cratons. *Bulletin of the Geological Society of Denmark* **39**, 213–28.
- Wolf MB and Wyllie PJ** (1994) Dehydration-melting of amphibolite at 10 kbar; the effects of temperature and time. *Contributions to Mineralogy and Petrology* **115**, 369–83.
- Zellmer GF, Rubin KH, Grönvold K and Jurado-Chichay Z** (2008) On the recent bimodal magmatic processes and their rates in the Torfajökull-Veidivötn area, Iceland. *Earth and Planetary Science Letters* **269**, 388–98.
- Zhu B, Peate DW, Guo Z and Liu R** (2017) Crustally derived granites in Dali, SW China: new constraints on silicic magmatism of the Central Emeishan large igneous province. *International Journal of Earth Sciences* **106**, 2503–25.